THESIS WORK FOR DUAL MASTER'S DEGREE

ITBA Mag. in Energy and Environment

KIT MSc. in Mechanical Engineering

ANALYSIS AND EVALUATION OF MONIKA'S FIRST RESULTS IN BYPASS CONFIGURATION

Luciano Javier Gardella
Industrial Designer
Facultad de Arquitectura Diseño y Urbanismo - UBA

Tutor
Prof. Dr. Ing. Thomas Schulenberg, KIT, ITES

Co-Tutor
Dipl.-Ing. Hans-Joachim Wiemer

Examiners
Prof. Dr. Ing. Thomas Schulenberg (ITES/KIT)
Prof. Dr. Ing. Andreas Class (ITES/KIT)
Dr. Ing. Cecilia Smoglie (ITBA)

Karlsruhe
10/05/2020

Declaration by author

I declare that I have developed and written the enclosed Master Thesis completely by myself and have not used any sources or means without declaration in the text. All thoughts from others and literal quotations are clearly marked. The Master Thesis was not used in the same or in a similar version to achieve an academic grading nor to be published elsewhere.

10.05.2020 

Date Signature

Acknowledgement

This work is the conclusion of a step in my academic and professional life. It would not be possible to achieve without the support and encouragement of people to whom I want to express my gratitude.

To my thesis director Prof. Dr.-Ing. Thomas Schulenberg and Dipl. Ing. Hans-Joachim Wiemer for their time, effort and dedication. And for the opportunity to do this work with them at the ITES. In this point, I would like to thank especially to Dr. Cecilia Smoglie for her guidance and for giving me the opportunity to start this process and open the doors of ITBA.

To my friends and colleagues Mariano Fosatti, Gaston Bisio, Juan Pablo D'Agnillo, Kevin Redosado and Marco Ordoñez. For their warmth and support throughout this adventure.

Finally, I want to show all my thanks to my family, for the patience and help from a distance. Without the love and support that you give me to afront the difficulties I would not have come this far.

Abstract

Analysis and Evaluation of MoNiKa's first results using GESI

The aim of this thesis is to show, discuss, and evaluate the results of MoNiKa Power Plant in stationary regime working at different part load in bypass operation. The experiment performed for this thesis during winter semester 2019, are the first results to come out of the facility. MoNiKa was authorised to operate at the end of 2018, and today is still under development.

The current work, will study the power plant to define its actual situation. The main issues to answer was the question of the reliability and accuracy of the measured data. Defining the degree of reliability of the measurements, is essential in order to have a starting point to carry out a correct evaluation of the facility. As well as the boundary conditions and the operational limits of the power plant. Each test performed in this work contributes to having a better understanding of the facility and its components. Furthermore, it contributes to build the *knowhow* of MoNiKa. And it will determine the base for the next steps in the research.

A software developed by the institute was the primary tool used to analyse the information obtained from the facility. GESI (Geothermal Simulation). Definition of the input needs to match the model to the facility was part of the challenge in this work too.

The comparison of the results from MoNiKa with GESI becomes a feedback process. Where at the end of each step, a better understanding of the facility was obtained. As a result, the whole prosses, the power plant was studied in deep, and a module of GESI was developed to simulate futures scenarios of MoNiKa.

Resumen

Análisis y evaluación de los primeros resultados del MoNiKa usando GESI

El objetivo de esta tesis es mostrar, discutir y evaluar los resultados de la Central Eléctrica MoNiKa en régimen estacionario trabajando con diferentes partes de carga en operación de bypass. Los experimentos realizados para esta tesis durante el semestre de invierno de 2019, son los primeros resultados que salen de la instalación. MoNiKa fue autorizada para operar a finales de 2018, y hoy en día sigue en desarrollo.

El trabajo actual, estudiará la planta de energía para definir su situación real. Las principales cuestiones a responder fueron la cuestión de la fiabilidad y la precisión de los datos medidos. Definir el grado de fiabilidad de las mediciones, es esencial para tener un punto de partida para llevar a cabo una correcta evaluación de la instalación. Así como las condiciones límite y los límites operacionales de la central. Cada prueba realizada en este trabajo contribuye a tener una mejor comprensión de la instalación y sus componentes. Además, contribuye a construir el conocimiento del MoNiKa. Y determinará la base para los próximos pasos de la investigación.

Un software desarrollado por el instituto fue la principal herramienta utilizada para analizar la información obtenida de la instalación. GESI (Simulación Geotérmica). La definición de las necesidades de entrada para hacer coincidir el modelo con la instalación fue parte del desafío en este trabajo también.

La comparación de los resultados del MoNiKa con el GESI se convierte en un proceso de retroalimentación. Donde al final de cada paso, se obtuvo una mejor comprensión de la instalación. Como resultado, se estudió en profundidad toda la prosa, la central eléctrica, y se desarrolló un módulo de GESI para simular futuros escenarios de MoNiKa.

Kurzfassungt

Analyse und Bewertung der ersten Ergebnisse von MoNiKa mit GESI

Das Ziel dieser Arbeit ist es, die Ergebnisse des MoNiKa-Kraftwerks im stationären Regime bei unterschiedlicher Teillast im Bypassbetrieb zu zeigen, zu diskutieren und zu bewerten. Die für diese Arbeit im Wintersemester 2019 durchgeführten Experimente sind die ersten Ergebnisse, die aus der Anlage hervorgehen. MoNiKa wurde Ende 2018 für den Betrieb zugelassen und befindet sich heute noch in der Entwicklung.

Im Rahmen der laufenden Arbeiten soll das Kraftwerk untersucht werden, um seinen Ist-Zustand zu definieren. Die wichtigsten Fragen, die es zu beantworten galt, waren die Frage nach der Zuverlässigkeit und Genauigkeit der gemessenen Daten. Die Definition des Zuverlässigkeitsgrades der Messungen ist unerlässlich, um einen Ausgangspunkt für eine korrekte Bewertung der Anlage zu haben. Sowie die Randbedingungen und die Betriebsgrenzen des Kraftwerks. Jeder in dieser Arbeit durchgeführte Versuch trägt zu einem besseren Verständnis der Anlage und ihrer Komponenten bei. Darüber hinaus trägt er zum Aufbau des Know-hows von MoNiKa bei. Und er wird die Grundlage für die nächsten Schritte in der Forschung bestimmen.

Eine vom Institut entwickelte Software war das Hauptwerkzeug zur Analyse der von der Anlage erhaltenen Informationen. GESI (Geothermische Simulation). Die Definition der Eingabebedürfnisse, um das Modell an die Anlage anzupassen, war auch bei dieser Arbeit Teil der Herausforderung.

Der Vergleich der Ergebnisse von MoNiKa mit GESI wird zu einem Feedback-Prozess. Am Ende jedes Schrittes wurde ein besseres Verständnis der Anlage erreicht. Infolgedessen wurde der gesamte Prozess, das Kraftwerk eingehend untersucht und ein Modul der GESI entwickelt, um Zukunftsszenarien von MoNiKa zu simulieren.

Index

List of figures

List of tables

List of symbols

Sym.	Description	Unit
A	Area	m^2
d	Diameter	m
d_H	Hydraulic diameter	m
Δl	Characteristic lengt	m
g	Gravity constant	m/s
$\dot{m}$	Mass flow	kg/s
$\dot{V}$	Volumen flow	m^3/s
ω	Angular velocity	RPM
k	Overall heat transfer coefficient	$kW/m^2{\cdot}K$
α	heat convection coefficient	$kW/m^2{\cdot}K$
Q	Heat	kJ
$\dot{q}$	Heat flux	kW
W	Work	kJ
P	Power	kW
η	Efficiency	%
cp	Specific heat capacity	kJ/kg·K
p	Pressure	MPa
Δp	Pressure loss	MPa
T	Temperature	°C
ΔT	Temperature diference	K
h	Specific enthalpy	kJ/kg
ρ	Density	kg/m^3
s	Specific entropy	kJ/kg·K
e	Internal energy	kJ/kg
x	Quality	%
μ	Dynamic viscosity	μPa-s
λ	Thermal conductivity	kW/m·K
K	Pressure loss coefficient	-
f	Friction factor	-
k_e	Relative roughness	-
ε	Absolute roughness	m
δ	Uncertainly	
$\bar{X}$	Average	
σ	Standard Deviation	
$\sigma_{\bar{X}}$	Standard Deviation of the Mean	

	Dimensionless numbers
Re	Reynolds
Nu	Nusselt
Pr	Prandtl

	Suffix
ORC	Organic rankine cycle
critic	Refers to critical point of the fluid
tw	Termal water
prop	Propane
Amb	Ambient
Point [1]	Outlet condenser – Inlet pump
Point [2]	Outlet pump – Inlet heat exchanger
Point [3]	Outlet heat exchanger – Inlet valve
Point [4]	Outlet valve – Inlet condenser
l	Length
i	Inner
o	Outer
in	Inlet
out	Outlet
isen	Isentropic
s	Isentropic prosses
th	Thermal
hyd	Hydraulic
ds	Design
*	Estimated value

1 Introduction

1.1 Geothermal energy - Background

The Paris agreement, during the 21st Conference of the Parties (COP 21) of the UNFCCC in December 2015, represents a framework in the policies to combat climate change. The main objective of the Agreement is to limit the temperature increase in this century to levels significantly below 2ºC. The high level of adherence by countries (approved by 195 of them) indicates that the world intends to develop a low-carbon economy. [1] In this context, renewable energies are the key to changing the energy matrix for a clean and emission-free one. Several technologies are currently in use and continue to be developed, improving their performance. Geothermal energy is one of them.

Geothermal energy is a renewable energy source that uses a hot fluid (usually steam and water) from a geothermal reservoir located in some underground layer of the earth. This fluid is used to provide energy, electricity or heat, and then it is reinjected into the geothermal reservoir. There it is reheated and can be used again to complete the cycle. In this way, it is a source of renewable energy. These plants do not only have the benefit that they do not need to burn fossil fuels to operate, but also eliminate the need for transport and storage of fuel. This characteristic means that the cost of producing energy is much lower than in a coal plant, but the investment to install a geothermal plant is much higher. Compared to other renewable energies, it has the advantage of not being intermittent. Geothermal energy offers a constant flow of energy production throughout the year because it does not depend on seasonal variations such as rain, river flows, wind, or the sun, as is the case of the others renewables technologies. [2]

It is important to distinguish between three types of geothermal energy plants. Firstly, Dry Steam Power Plants. These use steam released from underground sources to drive turbines and generate electricity. Although dry steam plants are simple to operate, they are limited by the few locations that produce enough steam for a commercial-scale plant.

Second, Flash Power Plants are the most common ones. They use long pipelines that extend to deep underground reservoirs, where the extreme pressure allows the water to remain liquid above its surface boiling point. The high-pressure water is pumped from the reservoirs. Then the fluid is expended, the water quickly turns into vapour (flash) and is used to drive a turbine. The surplus liquid water and the condensed steam are reinjected into the reservoir again, making the process sustainable.

Finally, Binary Cycle Power Plant: they represent the state of the art. This technology opens the possibilities to operate in areas with a reservoir temperature much lower than that required by other plants (low enthalpy supplies). Moderately hot water is taken from underground reservoirs, but due to the low temperature of the water, it is not possible to obtain energy directly. Another a fluid with a lower boiling temperature than the thermal water temperature is needed. Through heat exchanger, the thermal water evaporates the other fluid, which is used to drive a turbine and generate electricity.

1.2 Organic Rankine Cycle

Organic Rankine Cycles (ORCs) are power generation cycles which operate in the same way as conventional steam power cycles, but instead of using water, they use an organic fluid (such as a refrigerant or hydrocarbon). This was an important innovation that has allowed cycles to produce energy from low enthalpy sources (temperatures between 100°C - 200°C). While typical steam power cycles look for the higher temperatures and pressures in order to obtain the best efficiency possible, some applications are limited to a lower temperature. The ORC is one of the promising cycles that can be used to extract thermal energy from various energy sources that may only provide a source at a limited temperature, e.g.: Thermal water from a geothermal reservoir, heat obtain by a solar-thermal installation, exhaust gas from the combustion of a bio-material, or heat recovery applications from energy-intensive industries.[3] Thus, its use for the recovery of industrial waste heat is considered a measure of energy saving and efficiency that could contribute numerous benefits (energy, environmental and economic).

The strength of the ORC technology is its modular feature: a similar ORC system can be used, with little modifications, in conjunction with various heat sources. Furthermore, the main difference between conventional power cycles is that this technology allows a local and small-scale power generation. Today's range of application is from the kW to the MW scale.

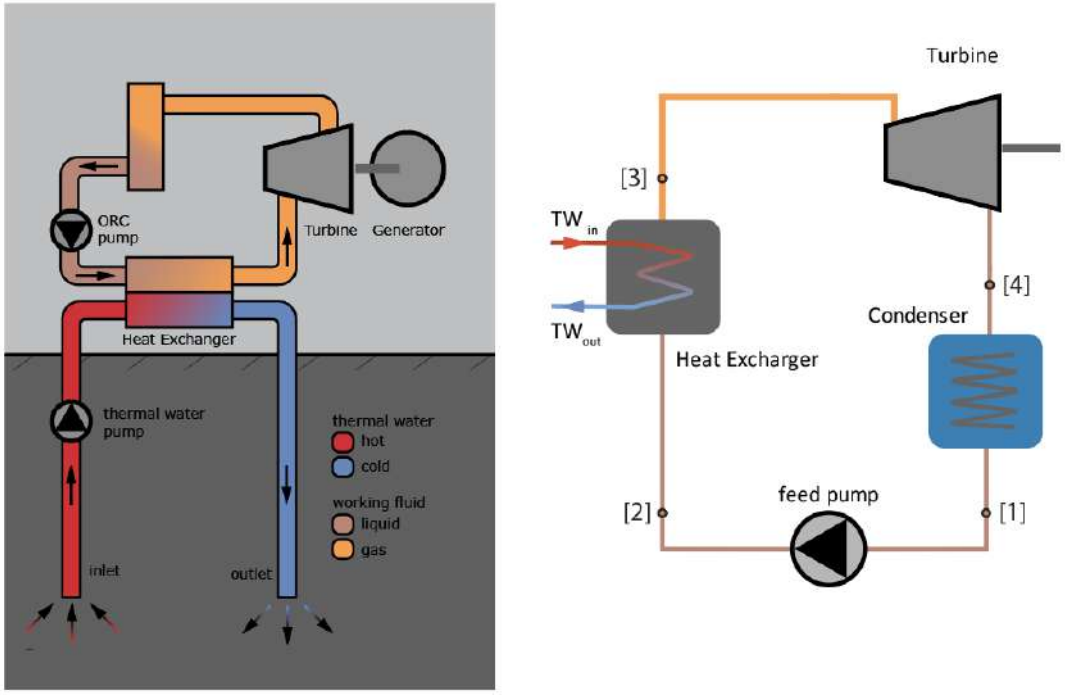

Figure 1: Illustration of Binary Plant setup

The Organic Rankine Cycle involves the same main components as a conventional steam power plant (a boiler, a work-producing expansion device, a condenser and a pump). The organic fluid (with high pressure) circulates through the *heat exchanger* (or evaporator), where the heat from the thermal water is transferred to it. Then the fluid is expanded in the *turbine*, which is connected to an electrical generator. The working fluid that gets out of the turbine with low pressure and

temperature is condensed in the *condenser*. Finally, its pressure is increased again with the *feed pump*, and the cycle starts again. In some cases, depending on the working fluid and the design of the ORC cycle, a higher thermal efficiency can be obtained by integrating a regenerating process to the cycle.

In addition to these components, a real ORC incorporates other equipment, like tanks to manage the mass flow, sensors used to measure and check the installation behaviour and provide a feedback to the control systems, piping and insulation. All these components are essential in real implementations and conform a mayor network of interactions that generate a mayor order of complexity of the facility.

As it was mention, binary power plants use an organic fluid instead of water as working medium. These fluids have the main property that they have a lower evaporation pressure and temperature than water, which makes them the key for low enthalpy heat sources power plants. Choosing the right one is the start point for designing an ORC process. The first rough approach is to define the critical temperature of the working fluid (which is related to the heat source temperature). Once the working fluid is selected, it will determine the installation setup.

Another important factor to consider at the design of an ORC plant is the type of cycle that the working fluid will perform: there are two main types of cycles. Subcritical cycles, where the working pressure is lower than the critical pressure of the fluid. The heating process occurs in the two-phase region. And supercritical cycles, in which the evaporation occurs above the two-phase region (the pump provides the fluid with a pressure higher than its' critical pressure) (*Figure 2, center and right,* comparison of both cycles under the same boundary conditions). This type of cycle is in focus of the new binary cycle power plant research. The supercritical process has a potentially higher gross power output than the subcritical ones (the enthalpy difference h_3-h_4 is usually higher). Almost 40% of gross performance increase is possible to achieve, depending on the fluid characteristics. This maximum occurs when the working fluid has a critical temperature ~0.8 times the respective geothermal water temperature. This association between the local geothermal temperature and the optimum critical temperature has to be one criterion for the selection of the working fluid. [4].

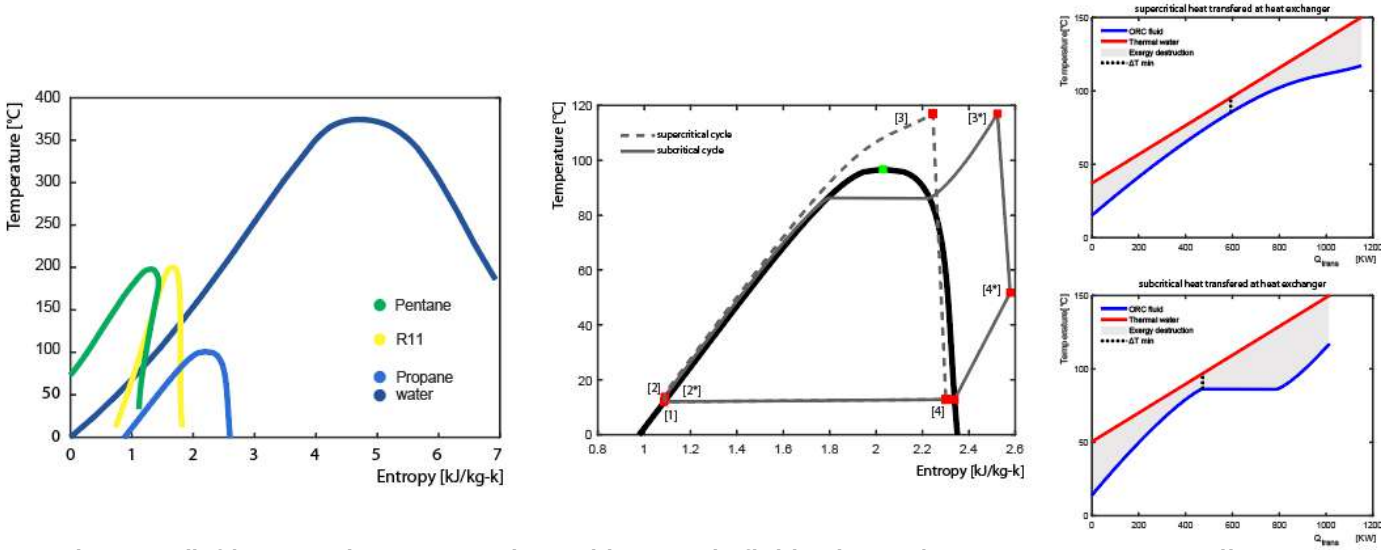

Figure 2: *(left)* Comparison or wet, dry and isentropic fluids. *(center)* Temperature-entropy diagram comparison subcritical [1-2*-3*-4*] and supercritical cycle [1-2-3-4]. *(right*) T-Q comparison of heat transferred at the heat exchanger *(up)* subcritical, *(down)* supercritical cycle

The second step for choosing the working fluid is the gradient of its saturated vapour curve in a T-s diagram. Fluids classified as dry (e.g. pentane) have a positive gradient, wet (e.g. water/propane) has a negative gradient, and isentropic fluids (e.g. R11) have a vertical gradient. This characteristic determines where the fluid's expansion will end. In dry and isentropic fluids, the expansion ends in the superheated region. Therefore, the fluid still has useable content of energy after the expansion. In this case, an internal heat recovery is possible. It can be placed before the condenser to preheat the fluid before it gets evaporated. While, wet fluids, the expansion takes place into the two phases region, in this situation is essential to check the vapor quality of the fluid after the expansion to prevent liquid droplets forming that can damage the turbine blades.

Others criteria that should be taken into consideration for choosing the working fluid are the environmental and operational ones. Such as high thermal conductibility, low specific volume, high chemical stability, low corrosiveness, low flammability, toxicity, low Ozone Depletion Potential (ODP) and Global Warming Potential (GWP). [4]

2 MoNiKa power plant

This chapter performs a descriptive analysis of the facility. The focus is on explaining the design of the ORC cycle and giving a detailed image of the characteristics that make up the power plant.

2.1 Design of MoNiKa ORC

MoNiKa (Modular low-temperature cycle Karlsruhe) is a facility built at KIT campus north with the idea of studying and optimizing the ORC process. This installation is a small and compact power plant. It was designed as a modular installation to allow the study and investigation of different components, focusing on the research of geothermal power generation from low-temperature heat sources [5].

The facility is a binary cycle, where the geothermal heat source is emulated. A hot water boiler heats the water at the site, which simulates the thermal water. The temperature and the mass flow on the water cycle can be modified to have a range of input conditions and emulate different scenarios.

The designed ORC cycle is a supercritical process; live steam parameters of 5.5 MPa and 117 °C can be achieved using propane as working fluid (P_{cric} = 4.25 MPa and T_{cric} 96.74 °C). Previous investigations showed that a supercritical ORC process has higher performance that subcritical ones. Therefore this installation is designed to work with a supercritical cycle. [4, 6] These investigations shall confirm too, that propane is a good option for ORC supercritical cycles. It shall achieve a specific net power output of 36.8 kW/kg and a thermal efficiency of 10.1% at supercritical conditions. Even though propane is not the best option in performance and other fluids showed better features. Propane, however, presents many other advantages: it is inexpensive and available through local suppliers, it is more environmentally friendly compared to other working fluids and presents less toxicity than other options. Propane is also a wet fluid. Therefore, the cycle is designed such that the fluid will be expanded into the two-phase region to the condensing temperature. Which means that an internal heat recovery is not possible.

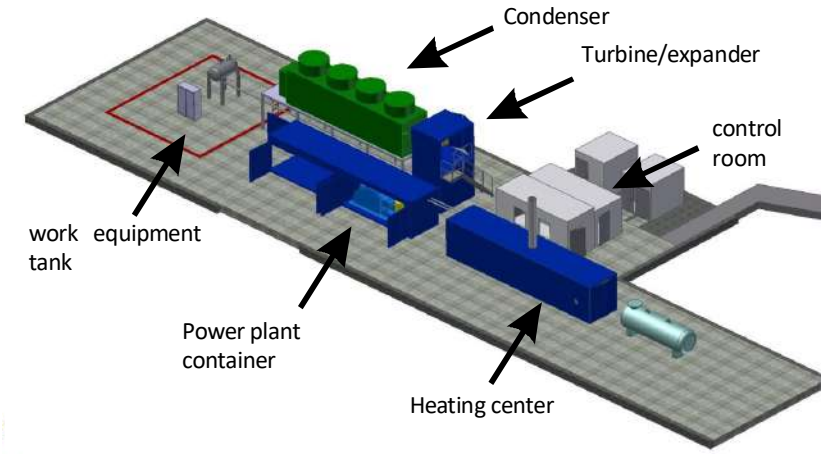

Figure 3:Illustration of MoNiKa Power Plant

2.2 Components description

The pumping system is compound by two pumps. The main pump is a LEWA triplex M514US G3G. It is a piston pump of max. 75 kW with a maximum mass flow of 3.6 kg/s and a design pressure of 6.5 MPa (in this will be referenced as main pump). This type of pumps has a high efficiency, and it can provide a mass flow independent from the outlet pressure. This characteristic confers a new degree of freedom and allows to work in many combinations of pressure and mass flow in the cases of part load. However, the experience shows that there was the possibility of having cavitation in the of the main pump. In an effort to avoid this situation, a support pump was installed. This is a centrifugal pump of max. 5.5 kW, manufactured by Grundfos, CRN20-04 E-FGJ-G-E (from now on it will be referenced as support pump).

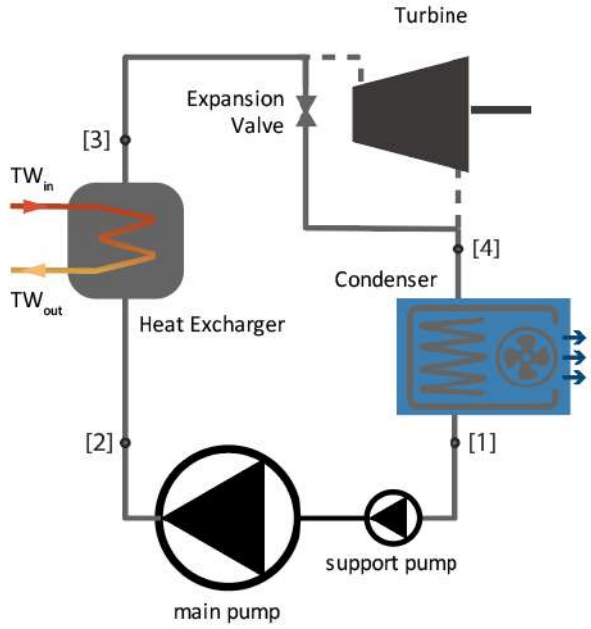

Figure 4: Illustration of Monika's main component setup

The heat exchanger manufactured by Gesmex, (from now on He Ex) is a vital component of the processes. It is the connection between both cycles, (thermal water and organic). It is a cross-flow heat exchanger designed to work in a subcritical and supercritical regimen. The device is formed by 200 circular welded plates grouped in 5 stage. It is all made from stainless steel (the plates and the casing). The design thermal power installed is 1000 kW for full load operation. And the working parameters for the water cycle are 0.7-1 MPa and 40-160°C (the geothermal fluid is projected to be liquid, there is no change of phase in this cycle). While in the propane cycle, the admitted pressures are from 5 to 6 MPa and the temperature range from 20 to 150°C.

The condenser manufactured by KÜHLTURMKARLSRUHE (from now on Cond.) is installed at 3.5 m of height. It is located between the exit of the turbine (or throttling valve), and the propane tank. However, the condenser is prepared to work with water spray. This option is not implemented at the date of this work. Therefore, this component is only analysed in dry configuration (the condenser uses ambient air as cooling fluid). The heat exchange areas are built symmetrically in "V"

configuration. They include three chambers. Each one is equipped with a vertical fan (impeller and diffusor) of 2.5m diameter. The power consumption of each motor is 13 kW, of power consumption at 322 RPM, and a maximum volume flow rate of 44 m^3/s each one (39 kW - 132 m^3/s total).

The last component of the circuit is the turbine, (Turb). The design requirements assumed an isentropic efficiency at full load of 0,8. and a vapour quality limit at the outlet of 0,9. However, this component is not analysed in this work. Instead, the aim is to study the cycle in bypass configuration. In order to set the installation in this way, three valves are implemented, two of them (11Y01 and 10YD4) have no implication in this works because they work just as open /close component to redirect the fluid while a Vetec valve (11PRV01), type 73,7 made the throttling process *(figure 5*

Figure 6*).* It is a rotary plug valve DN 80, made of stainless cast and carbon steel. The operational range of temperatures is from –100 to 400 °C and the maximum operational pressure is 16 MPa. At the facility, implementation of the control signal of the device is linear, that means that the percentage of the signal represents the same percentage of opening of the valve.

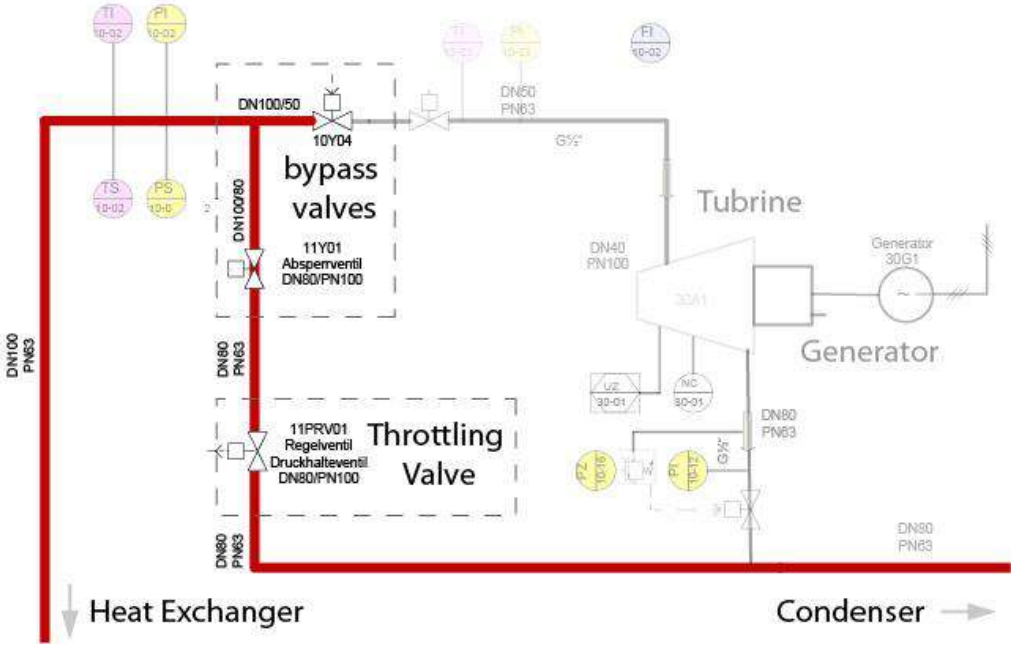

Figure 5: MoNiKa's schematic detail of bypass configuration

The *figure 6*

Figure 6 presents an overall view of MoNiKa's Power Plant. The photos show the main components involved in the ORC cycle. *(g)* shows the bypass configuration, the fluid direction in solid-line the bypass, while in dotted-line the fluid path for turbine's operation.

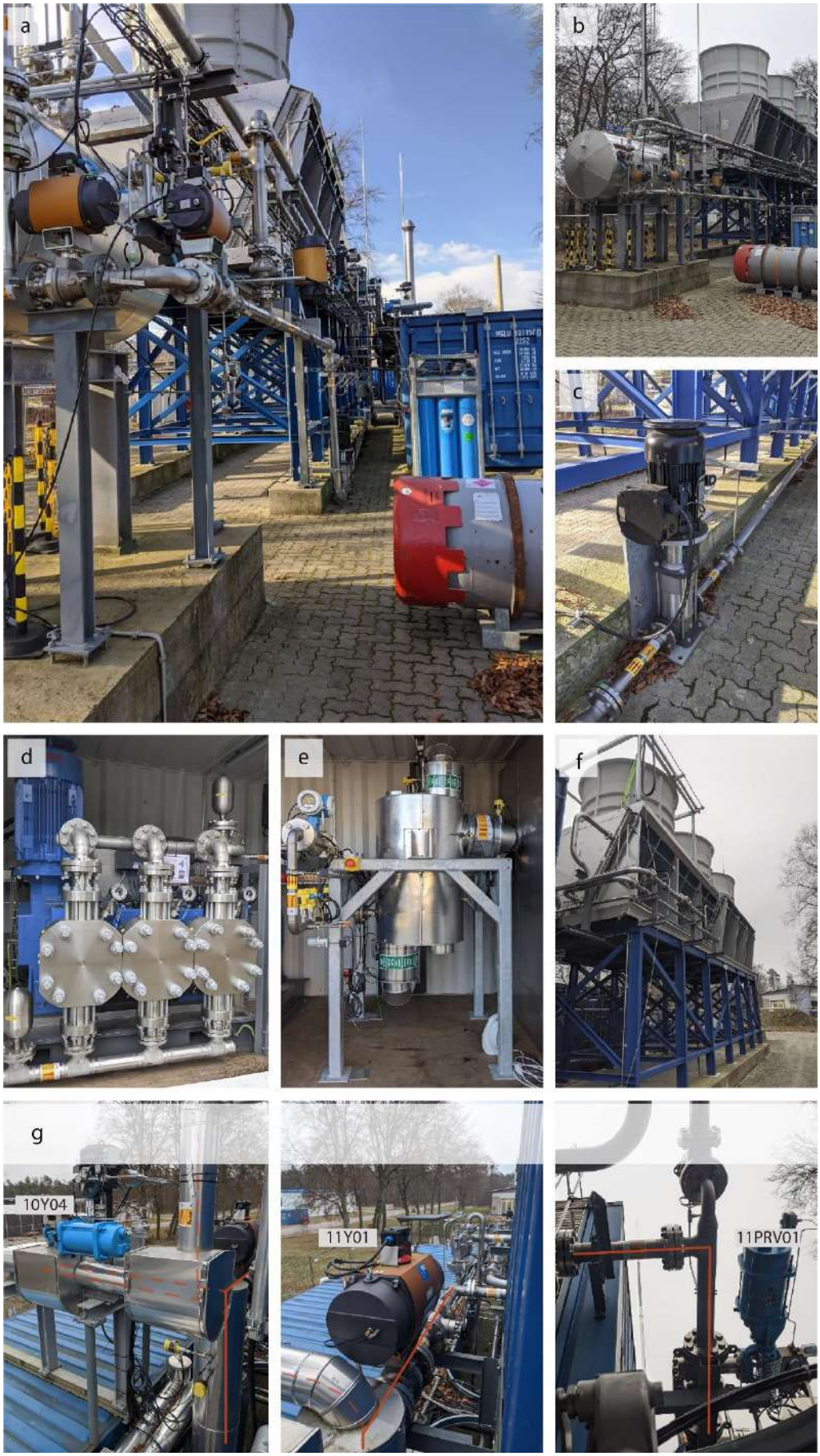

Figure 6 : Monika facility: *(a)* general photo of piping and components. *(b)* Propane tank, piping system and condenser. *(c)* Grundfos pump (d) LEWA pump, *(e)* Heat Exchanger. (f) Condenser. *(g)* bypass system pipes and valves

2.3 Full load operational point design

The ORC cycle can work under different boundary conditions. However, all of them are deviations of the designed full load point. This point is the optimum situation; it is where the power plant is using the maximum heat power available from the source, and it is working at full capacity. The intention is to run in this point the maximum time possible. Therefore, full load configuration is where all the components and the cycle in itself are optimized, and they work at their maximum efficiencies.

In the case of MoNiKa, the full load point is designed for a heat power of ~1000 kW. This is the heat that the thermal water has to release to the working fluid. The full load point of the thermal water cycle is defined at 2.4 kg/s mass flow rate of thermal fluid ($\dot{m}_{tw}$,), and the conditions at the inlet of the heat exchanger are: temperature ($T_{tw\ in}$) 150°C and pressure ($P_{tw\ in}$) 0.9Mpa.

In the ORC cycle, the mass flow rate of organic fluid is 2.9 kg/s ($\dot{m}_{ORC}$), and the design parameters of the working fluid at the inlet of the turbine are 117 °C at 5.5 MPa. The expansion of the working fluid is projected to be into the two-phases region, at a quality above 0.9 (in turbine operation). Different is the case in bypass operation, where the expansion of the fluid will occur outside the curve as superheat steam. In this case, there remains some useful energy, but it has to be released to the ambient via the condenser, since the MoNiKa cycle does not have a recuperator (*Figure 7 right* points[4-5]). In this work, the expansion will be considered as isenthalpic. (*Table 1*)

ORC Cycle	
Propane as Organic working fluid	
Live steam point [3]	5.5 MPa and 117 °C.
ORC mass flow	2.9 kg/s
Turbine isentropic efficiency	80%
Fluid quality (at the condenser inlet)	95%
Pumps isentropic efficiency	70%
Thermal Water Cycle	
mass flow	2.4 kg/s
Temperature in	150 °C
Temperature out	47 °C
Pressure in	0.9 Mpa
Power	
Thermal power:	~ 1000 kW
Heat released to the ambient	~ 930 kW
Gross Power generation	~ 150 kW
Net Power generation	~ 110 kW
Thermal efficiency	~ 15 %

Table 1 : MoNiKa's projected parameters at full load operational point in turbine operation [1-2-3-4*]

The *Figure 7* shows the simulation of the Monika's ORC cycle in GESI. The full load operational design point gives the boundary conditions, and some assumptions are taken into account to have a first approach to the cycle.

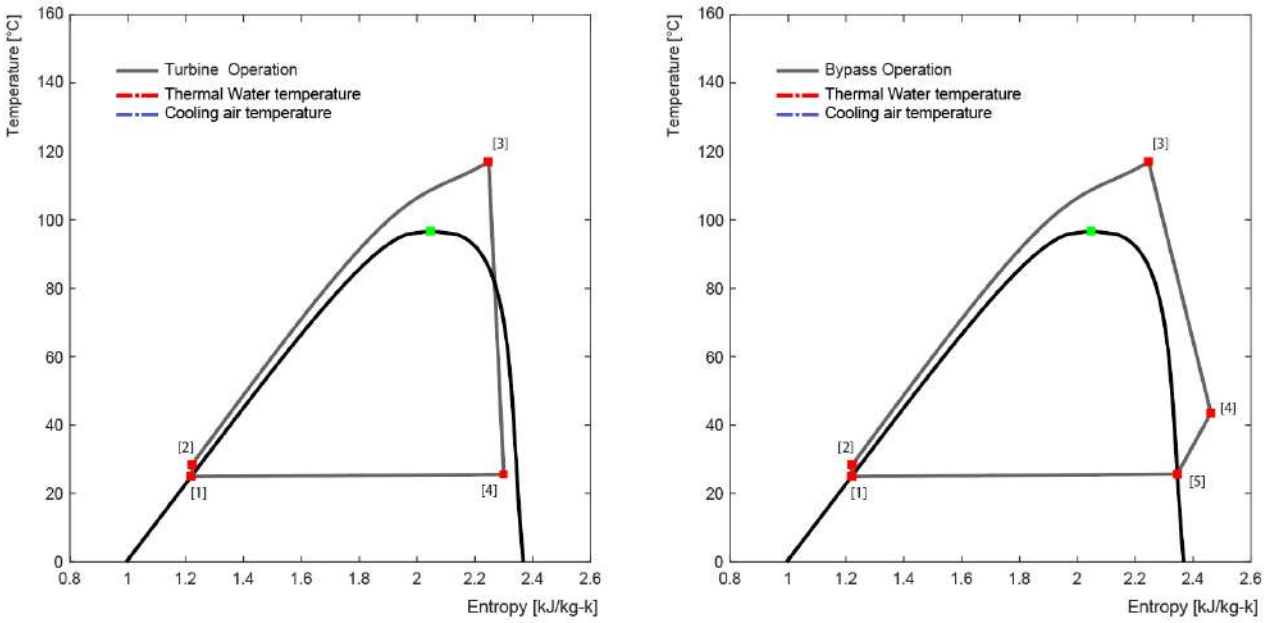

Figure 7: Temperature-Entropy graph of MoNiKa ORC design comparison (*left*) turbine operation (*right*) bypass operation

To fully define the cycle, the ambient temperature and therefore, the condensation temperature was estimated. The ambient temperature is 10 °C; Karlsruhe annual average temperature [7]. The condensation temperature considered is 25°C (15 °C above the ambient temperature. This was projected to be the optimum condensation temperature in order to maximize the Net Power generation of the cycle [4].

The pressure loss in the condenser has been provided by the manufacturer: 0.02 MPa. Since there was no information for the Heat Exchanger, the same value has been estimated. The values for the turbine and the pump isentropic efficiency is estimated from Christian Vetter work,(where the isentropic efficiency of the turbine is estimate in 0.8 and the pumps is 0.7 at full load). [8, 9]

Under this scenario, the power generation predictions are a gross power output (P_{Gross}) ~150 kW and net power output (P_{Net}) ~110 kW. However, these values cannot be verified in this work. In bypass configuration, the focus will be put instead on evaluation of the thermodynamic values at different points of the cycles (water and ORC), the heat transferred in the heat exchanger/condenser and the mass flow of all fluids (thermal water/propane/air).

From these designed and estimated values, a first and rough simulation is done of the MoNiKa's cycle. It is very theoretical, and it is based on many assumptions. However, this sets a starting point to study the facility. From the measurements and analyses of the data obtained from the tests, the theoretical model will be compared with the real one. On one hand, the simulations will be adapted to match the facility and to improve future predictions. On the other hand, they will study the deviations of the facility from the design parameters.

2.4 MoNiKa's instrumentation

The sensor system installed in MoNiKa meets two requirements: the first one as a power plant control system, the second one as a platform for investigations carried out at the plant. Therefore, the facility has installed more sensors that in a regular power plant along the whole cycle, i.e. at the inlet and outlet of each component *(Figure 8).*

The main indication measured are temperature and pressure at the inlet and outlet of each component (pumps, heat exchanger, throttling valve, condenser and propane tank). In many cases, the outlet of some component refers to the inlet of other one. But in other cases, the sensors are located at the ends of pipes, where pressure and heat losses are measured.

Mass flow rate and density of the working fluid are measures between the outlet of the main pump and the inlet of the heat exchanger using a Proline Promass 83F sensor. This sensor uses Coriolis forces and resonance frequency to have a direct measurement of the mass flow rate, the velocity and the density.

A WIKA TR34 class A PT100 is used to measure the temperatures in all the points of the facility. These sensors are resistance thermometer, with a range of operation is from -50 to 250 C. They are very compact, resistant to high vibration and give a fast response in time.

For pressure measurements, the sensors installed in MoNiKa are from VEGA: the models used are the Vegabar 81 and Vegabar 82. These pressures transmitters can be used universally for the measurement of gases, vapours and liquids. They have a ceramic measuring cell that allows the sensor to have a good performance in corrosive and hot environment. The main difference between bought sensors is the temperature range in which they can work. As a second observation, the pressure range that they exposed to work is not the same in all the ORC cycle, which causes that some measurements points have different accuracy than other ones.

The sensors are in direct contact with the fluid (propane and water). There is no sleeve or cap between them. This direct contact provides a better measurement of the fluid property, but it makes it impossible to remove the sensor from the pipeline without first emptying it. This is a big limitation, particularly in the ORC cycle, because this configuration does not allow to remove a sensor for performing a calibration test or to replace it in case of malfunction. Aware of this limitation, MoNiKa's measurement system is redundant. This means that in each measuring point, there are two or three sensors of the same kind installed. This configuration allows to have a *double-check* of the measurement. This is an important safety measure, if in case that some sensor fails.

For measure the ambient conditions, the plant is equipped with a Humidity and Temperature Transmitter (EE33 series) from where the conditions can be obtained in situ and do not depend on the weather stations. Furthermore, a set of thermocouple type k are installed in each chamber of the condenser. They are installed to measure the air conditions after the passing through the heat exchange areas, before the fan.

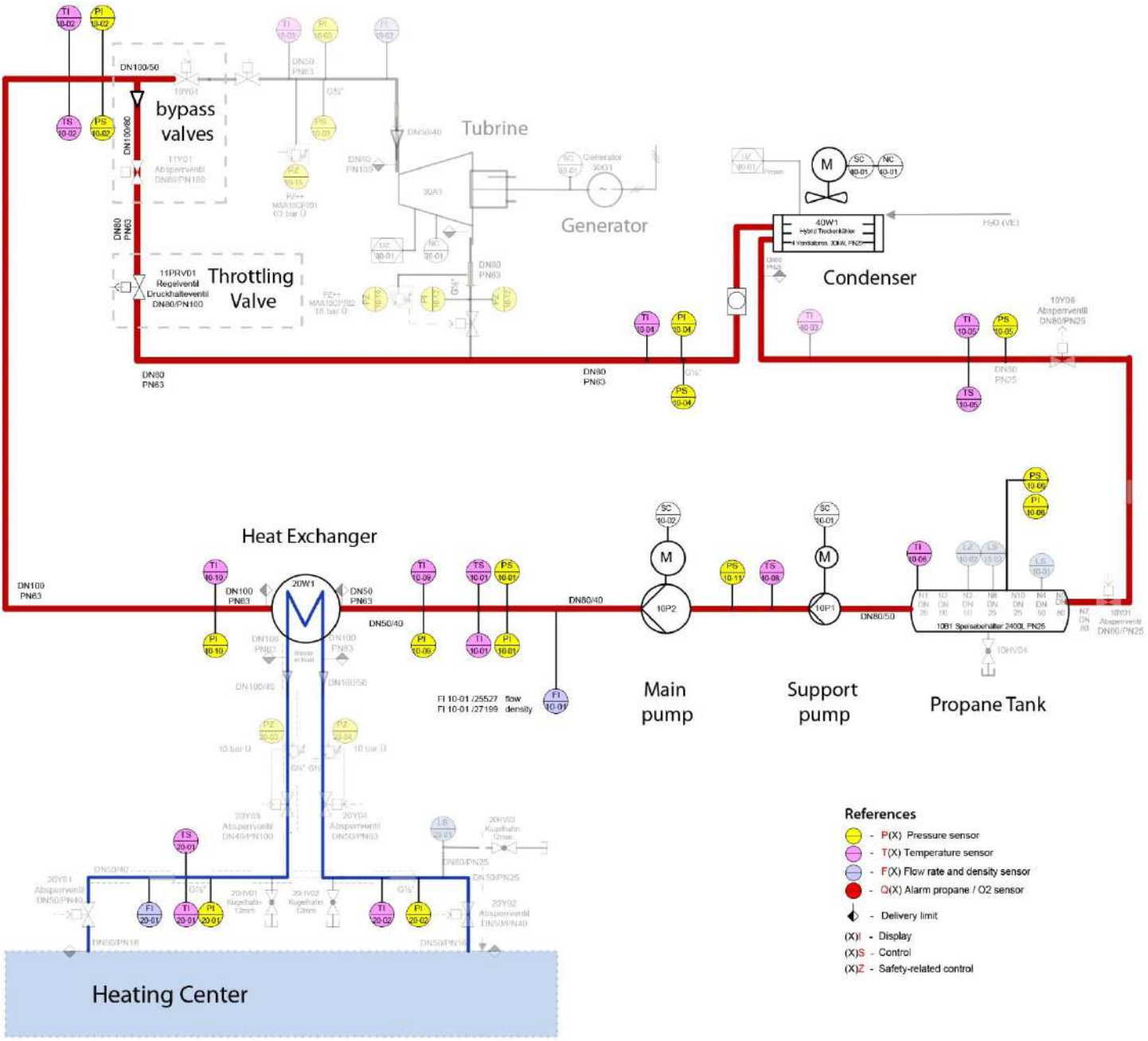

Figure 8: MoNiKa Power Plant schematic [9]

The

Figure 8 *8* shows a simplified schematic of Monika. Its shows the ORC and the thermal water cycle (red and blue) with all the main components and the sensors installed. All the secondary components and piping circuit where suppressed in order to have a clear imagen of the cycle, as well as the turbine loop. The sensor system is redundant. Where (X)I are display sensors used for operation of the power plant, and (X)S are for control. However, in this work, both types were used equally without discriminating their primary function.
In *Appendix Chapter*, the hole plant schematic is attached in case of needing more information of the cycle.

3 Theorical background

This chapter will discuss the theoretical background used in the study of MoNiKa. On one hand, it will show analyses with GESI, which is the primary tool used. It is essential to analyse and study the physical model that is implemented in GESI, how it works and have a good understanding of the limitations and assumptions that the software has. Furthermore, it is important to know what are the inputs that the software need, how are they implemented and the impact/sensitive of them in the simulations. On the other hand, the software cannot analyse and explain all the physical phenomena that occur in the facility. Therefore, it will be necessary to use some correlations to complement the study and deepen the analysis.

3.1 Energy balance

A balance of the energy E inside any component of the ORC can be written as: [10]

$$\frac{dE}{dt} = \dot{Q} - \dot{W} + \dot{m}_{in}\left(h + e_k + e_p\right)_{in} - \dot{m}_{out}\left(h + e_k + e_p\right)_{out} \qquad (3.1)$$

$$\text{kinetic energy} \qquad e_k = \frac{1}{2} V^2 \qquad (3.2)$$

$$\text{potential energy} \qquad e_p = gz \qquad (3.3)$$

Here, $\dot{Q}$ is the thermal power given from outside to this component, $\dot{W}$ is the mechanical power produced by this component, $\dot{m}$ is the mass flow, h is the enthalpy, V is the velocity and z the elevation at inlet and outlet each.

$$\text{stationary regime} \qquad \frac{dE}{dt} = 0 \;, \quad \dot{Q} = ct. \quad , \quad \dot{W} = ct. \qquad (3.4)$$

$$\text{mass conservation} \qquad \frac{dM}{dt} = 0 \quad , \quad \frac{dM}{dt} = \sum_{in} \dot{m} - \sum_{out} \dot{m} = 0 \qquad (3.5)$$

Under the steady-state condition, the time derivatives such as dE/dt and dM/dt are equal to 0 because there is no variation in the state variables. Additionally, the mass conservation statement

defines a constant mass flow. There is no filling or emptying process; the mass flow rate at the inlet is the same as the outlet.

3.2 GESI

GESI (Geothermal Simulation) [11] is an in-house program that has been developed in MATLAB by the ITES (Institute for Thermal Energy Technology and Safety) for studying and optimizing the thermodynamic process of the Organic Rankine Cycle (ORC). The software bases its calculus on the data taken from REFPROP, which is a fluid properties database from the National Institute of Standards and Technology. [12]

This tool simulates the ORC Power Plant in stationary regime by the selection of different organic fluids, definition of the thermal water values, selection of the operational points, the ambient characteristic and the equipment characteristics. It provides a main image of the whole process.

The version of the software that was used in this work is 2.3.6b version. It was validated by Christian Vetter via code-to-code comparison with IpsePro (Version 4.0, SimTech Simulation Technology) [13], and it showed a very good performance. "*The majority of the values show only a relative error of less than 0.02% and the absolute errors of the net power of the processes calculated in GESI corresponds to a relative error of less than 0.2%". [14]*

The software has different modules, focused on different power plant topologies and configurations. In this work, the main part of the analysis and the comparison of the data obtained from MoNiKa was using the **GESI-Rankine** and **GESI-Teillastreg module**, in which it is possible to calculate the cycle at full load and part load operation.

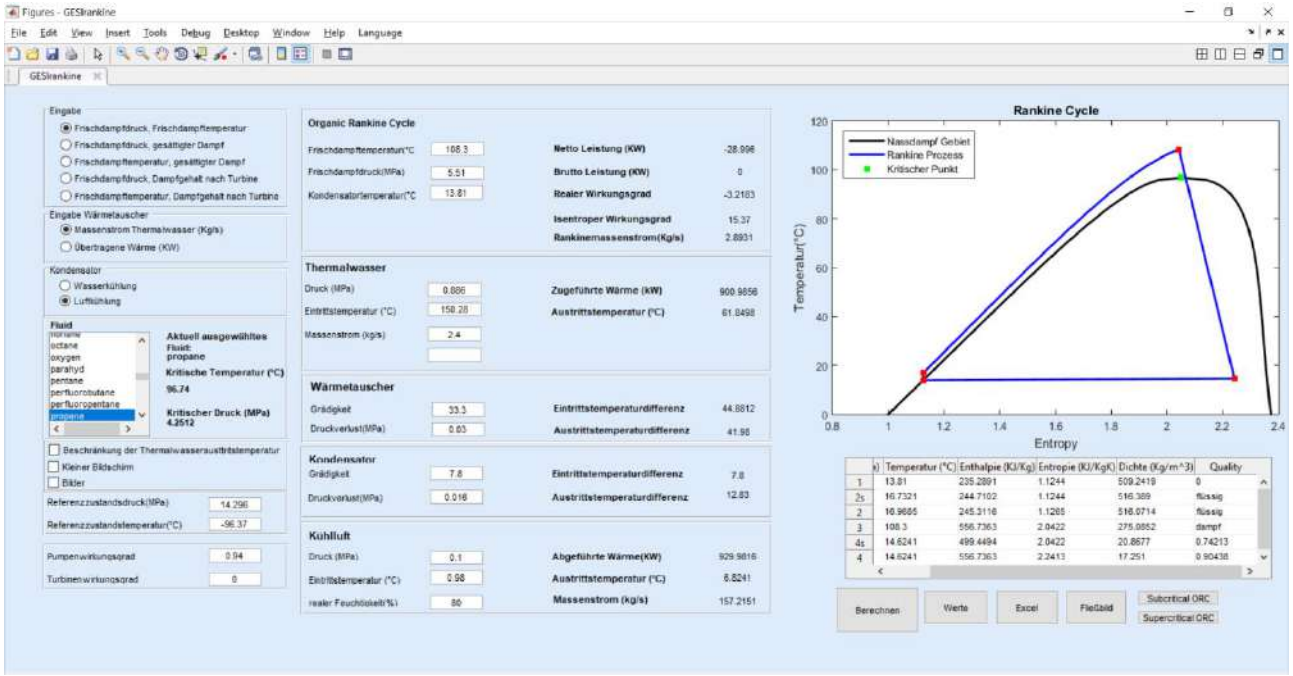

Figure 9: GESI-Rankine module

The *Figure 9* shows the graphical interface of the software. On one hand, the input data. This information provides input from three sources: ambient characteristics, ORC and thermal water cycle design and facility characteristics (

Table 2). On the other hand, the software calculates the mass flow of the working fluid, all thermodynamic states at the ORC points. GESI will generate different types of graphs to show the cycle (temperature-entropy, enthalpy-entropy, and temperature-heat$_{transfered}$ curves of the fluids in the heat exchanger/condenser). Furthermore, it calculates all the information related to the power of the cycle (net power, gross power and thermal efficiency).

Cycle Design		
Organic fluid used in the cycle		
Characteristic of one point		
	Point [3] of the cycle	Live steam pressure, live steam temperature
		Live steam pressure, saturated stem
		Live steam temperature, saturated stem
	Point [4] of the cycle	Live stem pressure vapor content after the turbine
		Live stem temperature vapor content after the turbine
Thermal Fluid		
	Pressure at the inlet of the Heat Exchanger	
	Temperature at the inlet of the Heat Exchanger	
	Mass flow of the thermal water / Heat delivered by the thermal water	
Facility Characteristics		
Heat Exchanger	Pressure loos of the ORC fluid	
	Minimal temperature differential (MTD)	
Condenser	Type of cooling fluid that will be use. Air/Water	
	Pressure loos of the ORC fluid	
	Minimal temperature differential (MTD)	
Pump	Isentropic efficiency	
Turbine	Isentropic efficiency	
Ambient		
Air as cooling fluid		
	Temperature	
	Pressure	
	Relative humility	

Table 2: GESI input parameters

GESI has many ways to define the ORC cycle and the boundary conditions. It is not part of this work to describe in detail all the options and configurations that the software offer. I will focus instead this analysis and explication in the way that the software was implemented in my thesis.

3.2.1 Modelling

GESI allows the simulation of subcritical and supercritical Organic Rankine Cycles. The main structure of the software starts from an ideal thermodynamic model. The ORC cycle is described by:

1 - 2: An Isentropic compression at the pump / supply of work to the cycle
2 - 3: isobaric supply of heat at the heat exchanger
3 - 4: isentropic expansion at the turbine / extraction of useful work from the cycle

4 - 1: isobaric removal of heat (condenser).

However, this ideal cycle cannot be achieved in reality. This way GESI contempt loses and efficiencies of the components in the calculations which are needed for a better estimation of the real case. The following description is the mainframe of equations that compound GESI's physical model. The explanation of the software logic and the assumptions made in it. [13]

In order to calculate the ORC, GESI will define the thermodynamic values of pressure (p), Temperature (T) density (δ), specific enthalpy (h), specific entropy (s) and the quality of the fluid (x). from the database of REFPROP using the subroutine *refropo.m.*

Determination of point [1] (Condenser outlet)

GESI defines this point from the condensation temperature (input) and assumes that, the organic fluid is on the saturation liquid line; it considers that in this point the vapour quality of the fluid is 0. From this assumption, it calculates all the thermodynamic values in this point

This assumption allows that this point can be defined by a single input, condensation Temperature (T_{cond}). However, it does not consider the possibility that supercooled liquid is present at the condenser outlet.

Determination of point [2] (Pump compression)

Given the point [1] and from the pressure value at the inlet of the turbine (point [3]), and the pressure losses in the Heat Exchanger (all inputs), the software calculates the pressure of the point [2]. Then calculates the thermodynamic values of the point [2s] (isentropic compression) and finally, using the isentropic efficiency of the pump ($\eta_{\,isen\,pump}$) define the values of the point [2].

The performance of the pump is calculated as follows:

$$\eta_{\,isen\,pump} = \frac{h_{2S} - h_1}{h_2 - h_1} \qquad (3.6)$$

$$P_{\,hyd} = \Delta p_{[2-1]} \cdot \dot{V} \qquad (3.7)$$

$$P_{\,pump} = \frac{P_{\,hyd}}{\eta_{\,isen\,pump}} \qquad (3.8)$$

A distinction is made between the hydraulic power $P_{\,hyd}$, which is the energy supplied to the fluid, calculate by the pressure difference at the inlet and outlet of the pump ($\Delta p_{[2-1]}$) and the volume flow rate ($\dot{V}$) and the pump power ($P_{\,pump}$), which is the energy required to drive the pump.

This model proposes an incomplete analysis of the power consumption of the pump. It is focused on the working fluid. It takes into account the effect of losses due to irreversibilities suffered by the fluid, but it does not consider the efficiency of the entire component: the efficiency of the frequency converter, motor and mechanics.

Determination of point [3] (Turbine inlet)

This is a given point; the pressure and temperature are inputs in the software. GESI uses REFPROP to calculate the other thermodynamic values of the point.

Determination of point [4] (Condenser inlet)

By defining the turbine isentropic efficiency ($\eta_{isen\ turb}$), the enthalpy at the turbine outlet can then be determined with real expansion. The program first sets the desired steam quality for the isentropic expansion state and gradually reduces it until the real relaxation state is reached.

In order to calculate this point, GESI uses the pressure of point [1], plus the pressure losses of the condenser: this determines the pressure at the point [4]. Then using the entropy from the point [3], it will define point [4s]. This corresponds to an ideal case of isentropic expansion of the fluid. Finally, using the isentropic efficiency of the turbine (input), the real expansion is calculated, point [4].

$$\eta_{isen\ turb} = \frac{h_3 - h_4}{h_3 - h_{4s}} \qquad (3.9)$$

Calculation of the unknown variables of the cycles

The following step in the software will be occurred in a subroutine named *hexblackbox*. This subroutine determinates the organic mass flow rate ($\dot{m}_{ORC}$), the heat transferred from the thermal water to the organic fluid (Q_{trans}), and the profile of temperatures curve of them. In order to calculate that, it will use the settings of the water cycle (input), the values calculate of points [2- 3] and the Minimal Temperature Difference at the heat exchanger ($MTD_{He\ Ex}$). The MTD is a design value that will determine the behaviour of the heat exchanger. This value has no influence on the thermal efficiency. However, the heat supplied to the process is strongly influenced by the MTD, which influences the mass flow of the ORC. Processes with propane showed a linear correlation between changes in MTD and net power output. [6]

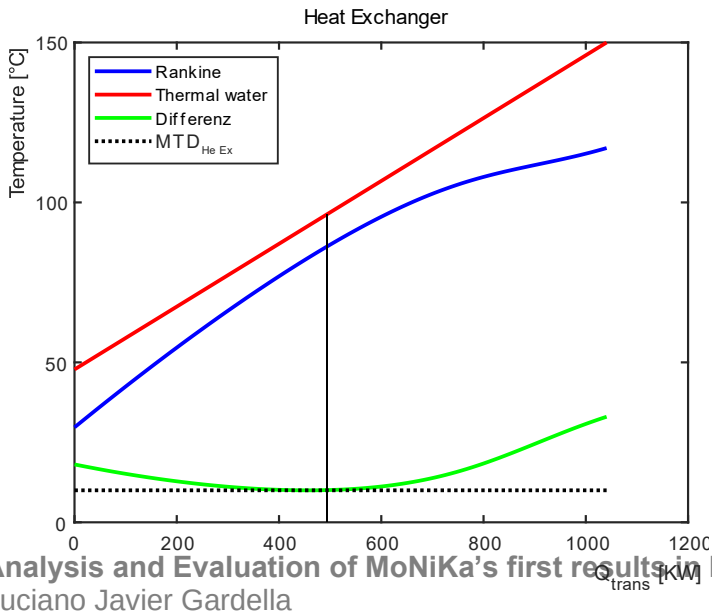

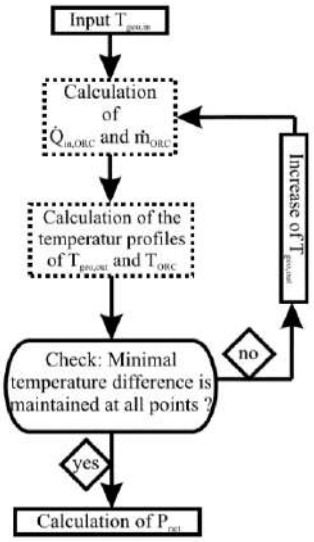

Figure 10: *(left)* Temperature-heat transfer diagram of the propane and the thermal water for full load first estimation (MTD He Ex = 10 K). *(right)* subroutine Iteration scheme. [14]

The subroutine calculates the maximum heat transfer possible but at the same time it will check that the temperature between both fluids never get lower than the defined value. The thermal water outlet temperature is not a design parameter. Therefore, the software has to estimate it ($T_{tw\ out}$) by the equation (*3.11*).

$$\Delta T_{min} = MTD_{He\ Ex} \tag{3.10}$$

$$T_{tw\ out,START} = T_3 + \Delta T_{min} \tag{3.11}$$

From the ORC points already calculated, the software defines the Q_{trans} in the heat exchanger *(equation (3.14)).* This heat is calculated with the *cp* of the water obtain from REFPROP as an average of the both temperatures. Finally, from equation (*3.15*) the ORC mass flow $\dot{m}_{ORC}$ is calculated.

$$\dot{Q}_{trans} = \dot{Q}_{tw} = \dot{Q}_{ORC\ in} \tag{3.12}$$

$$\dot{Q}_{tw} = \dot{m}_{tw} \cdot Cp_{tw} \cdot (T_{tw\ in} - T_{tw\ out}) = \dot{m}_{ORC} \cdot (h_3 - h_2) = \dot{Q}_{ORC\ in} \tag{3.13}$$

$$\dot{Q}_{trans} = \dot{m}_{tw} \cdot cp_{tw} \cdot (T_{tw\ in} - T_{tw\ out}) \tag{3.14}$$

$$\dot{Q}_{trans} = \dot{m}_{ORC} \cdot (h_3 - h_2) \tag{3.15}$$

Finally, the subroutine stars an iteration process *(figure 10 right)* to verified the MTD condition between both fluids. In case that this condition is broken in some point of the Q-T curves, the software increase $T_{tw\ out}$ and starts the prosses again.

GESI assumes that the device is an ideal insulated heat exchanger and that the heat losses to the environment can be neglected. The heat supplied by the thermal water is the same as the one absorbed by the ORC fluid.

The following step in GESI is calling the *condblackbox* subroutine. This is a similar process with using the same assumptions with the objective to calculate the mass flow and the temperature difference of the cooling fluid that in this work will always be ambient air. ($\dot{m}_{AIR}$ and $T_{AIR\ out}$).

$$T_{AIR\ in} = T_{Ambient} \tag{3.16}$$

$$\dot{Q}_{relased} = \dot{m}_{AIR} \cdot Cp_{AIR} \cdot (T_{AIR\ in} - T_{AIR\ out}) = \dot{m}_{ORC} \cdot (h_2 - h_1) \tag{3.17}$$

Overall parameters calculation

The thermal efficiency is an important value in order to compare the cycle with others and to make an estimation of its performance.

$$\eta_{th} = \frac{|q_{in}| - |q_{out}|}{|q_{in}|} = \frac{|w_{turbine}| - |w_{pump}|}{|q_{in}|} = \frac{(h_3 - h_4) - (h_2 - h_1)}{h_3 - h_2} \tag{3.18}$$

The efficiency is defined as the ratio of benefit to expenditure. The benefit is the turbine power minus the pump consumption. In the equation *(3.18)*, the other power consumers are considerate neglected, e.g. the power consumption of the condenser's fans or the power consumption of the pump of thermal water either.

$$P_{gross} = \dot{m}_{ORC} \cdot (h_3 - h_4) \tag{3.19}$$

$$P_{turb} = \dot{m}_{ORC} \cdot (h_3 - h_4) \cdot \eta_{isen\ turb} \tag{3.20}$$

$$P_{net\ out} = n_{th} \cdot \dot{Q}_{ORC\ in} \tag{3.21}$$

$$P_{net\ out} = \dot{m}_{ORC} \cdot [h_3 - h_4 - (h_2 - h_1)] - P_{fan} - P_{tw\ pump} \tag{3.22}$$

GESI will calculate the power parameters. the gross power generated by the ORC and the net Power. The net power is given by the gross power minus the power requirements of the pump and further auxiliaries. The pump power can also be calculated via the specific enthalpies. The most significant part of the auxiliaries power consumption are the fans of the cooler. Other system consumptions are neglected. However, in the actual version of GESI, P_{fan} and $P_{tw\ pump}$ are not considered in the calculations. Instead, it calculated the net power as.

$$P_{net\ out} = \dot{m}_{ORC} \cdot [h_3 - h_4 - (h_2 - h_1)] \tag{3.23}$$

For the direct comparison of the net power of different cycles, a new characteristic factor has been defined: The specific net power ($P_{net\ spec}$), indicates the net power which can be produced by a given geothermal fluid mass flow of 1 kg/s.

$$P_{net\ spec} = \frac{P_{net\ out}}{\dot{m}_{tw}} \tag{3.24}$$

3.3 Throttling

This thesis will study the MoNiKa at bypass configuration. In order to calculate that situation, the following assumptions were considered. The throttling as an adiabatic and isenthalpic process, where no work is done ($\Delta Q = 0 \quad ; \quad h_{in} = h_{out} \quad ; \quad W = 0$). [15, 16] With these assumptions, I could calculate this situation with GESI. The software calculates a throttling valve instead of a turbine by defining the isentropic efficiency equal to 0 ($\eta_{isen_{turb}} = 0$), without any further modifications at the code.

3.4 Heat and pressure losses

There are situations where the assumptions made by GESI do not correspond to the actual situation of the facility. The software does not contemplate the phenomena that occur in the piping lines. At this version, the software does not consider any pressure or heat losses from the outlet of one component to the inlet of other one. In some cases, this assumption has no influence (as the line between the main pump and the heat exchanger), but in other cases, it was necessary to correct this assumption.

In order to study the effects in the pipes, I developed a MATLAB code. Its main propose is to verify the measurements between the heat exchanger - throttling valve, and the condenser -main pump. The inputs correspond to the values of temperature, pressure and height at the inlet and outlet of the pipe, as well as the ambient conditions (temperature, pressure and air velocity). Using REFPROP and the following model and correlations, it estimates the heat and pressure losses. This Matlab function was developed for the particular case of MoNiKa piping system. It considers that the fluid is single-phase. Furthermore, in a previous check of the ORC Reynolds' number(*3.25*), it was detected that in all the cases studied, the fluid shows to have a turbulent behaviour, therefore this routine is focussed on this regime.

$$Re = \frac{\dot{m}\, d_H}{A\, \mu} \qquad (3.25)$$

The Reynolds' number is calculated as the ratio between the fluid mass flow $\dot{m}$, the hydraulic diameter d_H, (it will be consider to be equal to the inside diameter of the pipe), the internal cross area of the pipe A, and the dynamic viscosity μ of the fluid (REFPROP).

3.4.1 Pressure losses: Nikuradse correlation

The pressure loss is defined by the *Darcy–Weisbach equation*. Were K represents the pressure loss coefficient, in this approach only the losses that occur due to the length of the pipe will be taken in consideration, the local losses that occur in the components of the piping system , like inlets, bends and outlets, will not be taken in account, principally because they are not significant and in the pipe sections studied they are few of these components.

$$\Delta p = \frac{1}{2}\frac{K\,\dot{m}^2}{\rho\ A^2} \tag{3.26}$$

The pressure loss coefficient (*3.27*) depends on the friction factor f, the hydraulic diameter d_H, and the length of the pipe Δl.

$$K = \left(\frac{f\ \Delta l}{d_H}\right) \tag{3.27}$$

To define the friction factor for turbulent regime (Re > 4000) and rough tubes, the Nikuradse correlation is used. This correlation depends on the relative roughness (*3.29*), which is defined by the absolute roughness ε, and the inner diameter of the tube *d*. this information was obtained from the manufacturer datasheet.

$$f = \frac{1}{\left[2\ log\left(3.71\ \frac{d_H}{\varepsilon}\right)\right]^2} \tag{3.28}$$

$$k_e = \frac{\varepsilon}{d} \tag{3.29}$$

3.4.2 Heat losses: Dittus-Boelter correlation

The heat transfer is characterized by Fourier law (*3.30*). This will be used to calculate the heat flow from the ORC working fluid to the ambient through the pipe wall.

$$\dot{q} = k\ A\ \Delta T \tag{3.30}$$

Where q̇ is the heat flux transferred between both fluids trough the wall of the condenser, k is the overall heat transfer coefficient, A is the heat exchange area between both fluids and ΔT is the arithmetic mean temperature difference, defined in eq. (*3.31*) where $T_{p,in}$ and $T_{p,out}$ are the

$$\Delta T = \left(\frac{T_{p,in} + T_{p,out}}{2}\right) - T_{amb} \tag{3.31}$$

temperatures of the inlet and outlet of the propane, and T_{amb} corresponds to the ambient temperature. The product $\mathrm{k\,A}$ for pipes is defined as:

$$\frac{1}{k\,A} = \frac{1}{\alpha_i\,A_i} + \frac{(d_o - d_i)}{2\,\lambda_{pipe}\,A_i} + \frac{1}{\alpha_o\,\eta_o\,A_o} + Rf \qquad (3.32)$$

The first term in equation *(3.32)* refers to the heat convection inside the tube, in this case the convection in the propane, α_i is the inner heat transfer coefficient and A_i is the inner area of the pipe. The second one is the conduction inside the walls of the tube, it depends on the geometry (d_o and d_i are the outer and inner diameter) and properties of the material, λ_{pipe} is the thermal conductivity of the wall. The third term represents the convection outside the tube, in this study this term was simplified by taking the assumption that the outside temperature of the pipe is the ambient temperature. Rf is the fouling resistance. In this case, MoNiKa is a new facility and the working fluid do not allow the formation of biological organisms, so I neglected this term.

From the Nusselt number is the ratio of convective to conductive heat transfer at a boundary in a fluid. From it is possible to calculate the heat convection coefficient α:

$$Nu = \frac{\alpha\ d_H}{\lambda} \qquad (3.33)$$

In this case for estimating Nu, the Dittus-Boelter correlation *(3.34)* is used, valid for the ranges:

$0{,}7 < \mathrm{Pr} < 160, \quad \mathrm{Re} > 10000 \quad \text{and} \quad \mathrm{L/di} > 10$

$$Nu = 0.23\,Re^{0.8}\,Pr^{0.4} \qquad (3.34)$$

$$Pr = \frac{\mu\ c_p}{\lambda} \qquad (3.35)$$

This correlation describes the Nusselt number as a relationship between the Reynolds number *(3.25)* and the Prandtl number (*3.35*). This last dimensionless number is obtained from REFPROP. It is calculated from the input values.

4 Experimental uncertainty and error propagation

This chapter will discuss the accuracy of the measurements, which are the sources of systematic error that cause an offset from the true value, and the statistical analysis done to decrease the causes of random error which scatter around a mean value

4.1 Systematic error

A systematic error is one that occurs in the same way in all measurements. It may be caused by an instrument defect, in a particularity by the operator or by the measurement process. Systematic errors can be corrected or reduced in influence by calibrating the measuring system.

In this work, two sources of this type of error were identified. The first one is generated by the sensors, and it is defined by the accuracy of themselves. The other source is related to the stationary

conditions needed to take the measurements on the facility, and they are strongly affected by the environmental conditions and the thermal inertia of the installation.

4.1.1 Sensors measurement accuracy

In the case of the temperature as well as mass flow and density sensors, the calculation of its accuracy was straightforward to determine, using the information provided by the manufacturer in the datasheet of the product. These sensors have an accuracy related to the magnitude of the measurement that they are doing.

Magnitude	Model	Manufacturer	Measurement Range	Accuracy	Max Absolute error
Pressure	Vegabar81	Vega	0 to 10 MPa	0,2% of full range	0,02 MPa
Pressure	Vegabar82	Vega	0 to 10 MPa	0,1% of full range	0,01 Mpa
Pressure	Vegabar82	Vega	-1 to 10 MPa	0,1% of full range	0,01 Mpa
Pressure	Vegabar81	Vega	-1 to 2,5 MPa	0,2% of full range	0,005 MPa
Pressure	Vegabar82	Vega	-1 to 2,5 MPa	0,1 % of full range	0,003 Mpa
mass flow	Promass 83F	Endress +hauser	-	± [0,1+((0,0025/ṁ)*100)] * ṁ/100	0,005 kg/s
density	Promass 83F	Endress +hauser	-	±0,01	0,01 kg/L
Temperature	TR34 class A	WIKA	-50 to 250 °C	± 0,15 + 0,002 * | T | in [°C]	0,4 °C

Table 3: List of MoNiKa's types of sensors and accuracy

Different was the case of the pressure sensors. It was complicated to define the correct accuracy of the devices because I did not have the information about how they were calibrated. At first, some assumptions were taken in order to obtain information from the test, but they overestimated the accuracy, and the propagated error was too big. Finally, I could contact the manufacturer of the devices, and they were able to provide all the information from each one of the sensors (accuracy and calibration). The accuracy of these sensors is related to the range of scale that the sensor is calibrated to measure. Now this information is included in the MoNiKa's servers files [9].

The *Table 3* lists the different types of sensors installed in MoNiKa, and the *Figure 11* shows the place where they are located. The working fluid operational range defines maximum deviation of the sensors. On one hand, the pressure sensors' model depends on the working temperature and pressure range sated. Therefore, the accuracy of them is affected by the point of the ORC that they are installed. On the other hand, although the temperature sensors are the same model installed along the whole facility, its accuracy depends on the temperature of the measured value. Therefore, their maximum deviation will depend on the point installed too.

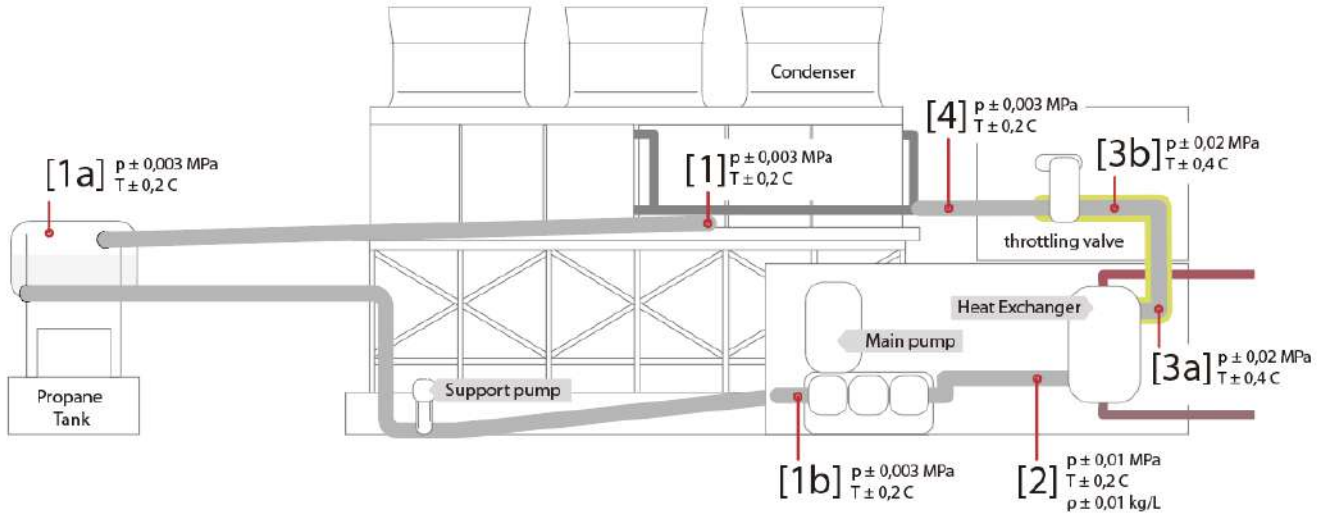

Figure 11: MoNiKa layout ORC cycle and sensors accuracy
p: pressure sensor, T: temperature sensor ,ρ density sensor

4.1.2 Data acquisition system accuracy

The data acquisition, as well as, the control system implemented in MoNiKa it's a standard protocol widely used in the industry: *"PROFIBU. It is a manufacturer-independent open field bus standard, of German origin, used for interconnection of simple input / output field devices with PLCs and PCs" [17]* .

At MoNiKa a SIEMENS SERIES S7-300 PLC is implemented as management of the system. The Analog input modules use to obtain the information from the sensors are S7331-7KF02-0AB0. This module converts the analog values from the sensor to digital values that are able to be processed by the PLC. This module has a high resolution and a high Common Mode Rejection Ratio. This means that the module will provide enough resolution to have an excellent lecture of the analog signal and will be able to filter all the induced noise. This is an important factor because all the information from the sensors works under HART protocol. This is a communication protocol that modulates the current from 4-20mA.

This module has a resolution of 14 bits (214 = 16384). This can be interpreted as an accuracy of ±0.001220703 mA. The uncertainty that the module adds to the measurements will be dismissed in this work. The magnitude of this is irrelevant compared with the accuracy of the sensors.

The Digital output module used to operate the expansion valve is 6ES73221BH010AA0. This case is similar to the one described for the analog sensors, where the resolution of the module is good enough to be dismissed. However, this does not imply that measurements obtained from the PROFIBUS server are free of uncertainty. It was determined that the accuracy of the drivers and the data acquisition system was good enough to be negligible. But in the case of the measurements obtained from the SIEMEMES SPPA-T3000 (MoNiKa's power plant control software), a statistical analysis is performed in order to estimate the accuracy of the data. As an example, power consumptions or transferred heat, are measurements without any information about the sensor's accuracy. In these cases, after exporting the measurements from the server, the standard deviation

of each parameter is calculated. Then the criteria of $2\sigma_x$ is used to define the typical confidence interval, 95,5 % of the population (this will be discussed in *chapter 4.2*).

4.1.3 REFPROP accuracy

REFPOP is a software developed by the National Institute of Standards and Technology (NIST). It is a powerful tool that calculates all the thermodynamic and transport properties of pure fluids and mixture substances. In this work, it is an essential resource at the moment of running the simulations on GESI, and to obtain the thermodynamic values from the measurements at MoNiKa. It is the only data table from where I obtained the information of all the fluids that were involved in the Rankine Cycle (Propane, water and air). This tool was fundamental for the aim of the thesis, and therefore it becomes essential to determine the error and influence of the software.

"*The REFPROP "database" is actually a program and does not contain any experimental information, aside from the critical and triple points of the pure fluids. The program uses equations for the thermodynamic and transport properties to calculate the state points of the fluid or mixture. These equations are the most accurate equations available worldwide. Their high accuracy is obtained through many coefficients in the equations, and thus the calculation speed will be slower than other equations such as the Peng-Robinson cubic equations. The equations are generally valid over the entire vapor and liquid regions of the fluid, including supercritical states; the upper temperature limit is usually near the point of decomposition of the fluid, and the upper pressure (or density) limit is defined by the melting line of the substance*". [18]

REFPROP accuracy depends on the length of the numbers that we set the software to work. In order to have a good resolution of the entropy and enthalpy values, it needs to work with 5 significant digits.

However, this is not the case in MoNiKa. The sensors installed there only allow to measure with 3 significant numbers of resolution. This situation skews the possible resolution of the REFPROP. When the software is seated to work under this limitation, a sensitive study of the variables showed that the uncertainly for temperature is ±0.2°C and ±0.002 MPa for pressure. In this scenario, the sensibility of the software is in the same range as the accuracy of the measurement sensors. This means that the accuracy of the software cannot be negligible, and it has to be taken into consideration in the calculation of the error propagation.

The uncertainty of the enthalpy and entropy derived from the measurements of temperature and pressure at MoNiKa can be expressed as follows [19]:

$$\delta h = \sqrt{\left(\frac{\partial h}{\partial P}\right)^2 \delta P + \left(\frac{\partial h}{\partial T}\right)^2 \delta T} \qquad (4.1)$$

$$\delta s = \sqrt{\left(\frac{\partial s}{\partial P}\right)^2 \delta P + \left(\frac{\partial s}{\partial T}\right)^2 \delta T} \qquad (4.2)$$

where δ is the uncertainty, and the first derivatives are estimated. In the case of the enthalpy, it is possible to be calculated using REFPROP. The software implements a module that calculates the partial derivate of the state properties dh/dT [P] and dh/dP [T]. In case of the entropy, this option is not implemented. The partial derivates were estimated, assuming that the pressure and temperature are independent variables, and the uncertain variation very small, that can be modelled with a linear function [20]. To trust in this method, I calculated the enthalpy uncertain in this way, and I compared this result with the ones calculated with REFPROP. The results indicated a generally good agreement with a deviation of 2%.

4.2 Random error

Random errors are measurements that fluctuate around a certain mean value. Although they are produced by variables not controlled in the experiment (they are not reproducible and thus cannot be corrected), their influence can be quantified by statistical procedures.

4.2.1 Statistical analysis

MoNiKa's PROFIBUS server allows us to export each parameter's value every one second. That generates a large dataset to analyse. In order to work with this amount of data, a statistic analysed is performed, following the European Standard: Requirements for measurement processes and measuring equipment (DIN ISO 10012:2003) and Basics of measurement technology (DIN 1319-1 and DIN 1319-3) [21, 22]. Furthermore, for define, some doubts at the moment of proceeding with the analysis, Evaluation of measurement data – Guide to expression of uncertainty in measurement JCGM (Joint Committee for Guides in Metrology) [23] was consulted.

Under the consideration of the central limit theorem, which establishes that, for large sample sizes, the sampling distribution of means approximates to a normal distribution even if the population distribution is not normal. I defined two protocols to obtain samples used in the study. The protocol depends on the type of test performed (cold run – hot run). In both cases, I was looking to obtain a larger population of measurements possible.

The system installed in MoNiKa has a measurement time cycle of 100ms. However, it is not possible to export the files with that resolution, it is limited to 1 measurement / 1s, 10s, 60s. The sever calculates the average of the range selected and export that value.

In cold run cases, from each valuable a time of 10 minutes of measurements was applied with a frequency of $1\ sample/sec$. That generated a population of 600 average measurements. While for the hot run, the protocol was $1\ sample/10\ sec$. and the time of measuring was of 1 hour. In this case the population generated was of 360 average measurements per valuable, (the hot run test is longer than the cold run, and applying the same time steps generates a big file that was not possible to export from the server). Although this population is smaller than in the cold run, in practice, this population is enough to assume a normal distribution.

From these populations ($\boldsymbol{N_i}$), and assuming this data is normally distributed, I calculate the Average ($\overline{\mathrm{X}}$) the Standard Deviation of the population ($\boldsymbol{\sigma_x}$), and finally, the Experimental Standard Deviation of the Mean ($\boldsymbol{\sigma_{\overline{X}}}$).

Population $$\mathrm{N} = \sum \mathrm{x}_1, \mathrm{x}_2, \mathrm{x}_3, \dots, \mathrm{x}_n \qquad (4.3)$$

Average $$\overline{\mathrm{X}}_\mathrm{i} = \frac{1}{\mathrm{n}} \sum_{\mathrm{k}=1}^{\mathrm{n}} \mathrm{X}_{\mathrm{i,k}} \qquad (4.4)$$

Population Standard Deviation $$\sigma = \sqrt{\frac{\sum_{\mathrm{i}=1}^{\mathrm{N}} (\mathrm{X}_\mathrm{i} - \overline{\mathrm{X}})^2}{\mathrm{N}-1}} \qquad (4.5)$$

Experimental Standard Deviation of the Mean $$\sigma_{\overline{\mathrm{X}}} = \frac{\sigma_\mathrm{x}}{\sqrt{\mathrm{N}}} \qquad (4.6)$$

The experimental standard deviation of the mean measures how far the sample mean of the data is likely to be from the real population mean. It quantifies how well $\overline{\mathrm{X}}$ estimates the measured value.

The standard deviation estimates the variability of the population from which the sample was drawn. It gives important information about how is the distribution of the population. A large standard deviation indicates that the data points can spread far from the mean and a small standard deviation indicates that they are clustered closely around the mean. Furthermore, the standard deviation can be used to use to determinate the accuracy of some measurement (*Figure 12*). As it was explained before, this method is used to determinate the accuracy of the measurements witch there is no information about the sensor.

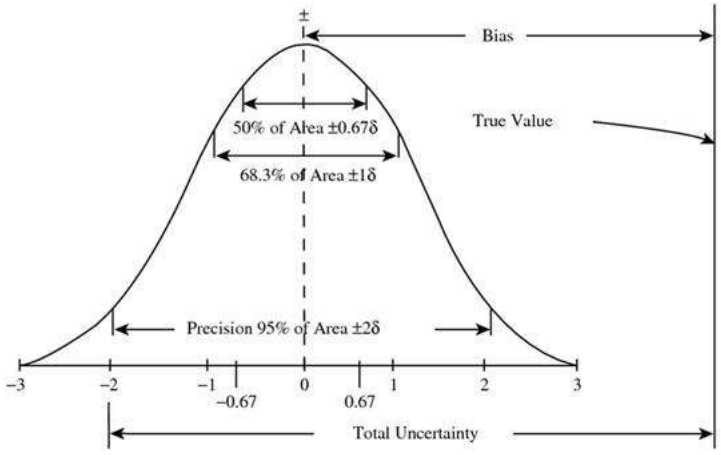

Figure 12: Normal distribution curve and error analysis. [24]

4.3 Error propagation

The general definition for the propagation of the uncertainly in a function $f(x, y)$, where x, y are independent variables and $\delta x, \delta y$ are the asocieated error of each variable is:

$$\delta f = \left|\frac{\partial f}{\partial x}\right| \cdot \delta x + \left|\frac{\partial f}{\partial y}\right| \cdot \delta y \tag{4.7}$$

$$f = A + B \qquad \frac{\delta f}{|f|} = \sqrt{\delta A^2 + \delta B^2} \tag{4.8}$$

$$f = A \cdot B \qquad \frac{\delta f}{|f|} = \sqrt{\left(\frac{\delta A}{A}\right)^2 + \left(\frac{\delta B}{B}\right)^2} \tag{4.9}$$

In this work, the functions involve such as the energy balance or the global parameters (Q_{trans} , P_{net} , P_{gross} , η_{th} , $\eta_{isen_{pump}}$, etc), are simple equations. The partial derivation can be calculated using simple functions as addition/subtraction (*4.8*) and multiplication/division (*4.9*).

5 Results

This chapter will describe the process and the decisions that were made throughout the thesis. It will explain what tests were made, under what criteria, and how the result conditioned the total work.

This work was performed under the protocol Rules for Safeguarding Good Scientific Practice at Karlsruhe Institute of Technology [25], all the experimental results were not altered in any aspect. The whole experimentation process tries to be as clear as possible to avoid any doubts of the results origin.

5.1 Test plan configuration

MoNiKa is a research installation that was finished at ends of 2018. This work is the first study performed on it. This is a new installation, and this study is the first one performed on it. The facility operates in a bypass configuration (the study of the turbine is beyond the scope of this thesis). This configuration it's a simplification of the cycle. Where the focus of the research is to study the overall cycle and all the components involves. This work will provide a base for futures research that will deepen knowledge about the MoNiKa plant.

Despite the fact that the facility is fully finished, all its components are installed and operative, at the day, some control loops of the control system are not fully optimized and automated. That implies that the most of the test runs were done manually controlled.

This condition involved a greater level of complexity. This work will not only be a study of the power plant. As well it will contribute to build the knowhow and earning practical experience in the operation of MoNiKa.

It was essential to design and project each test on MoNiKa. It was not possible to design and be ready to run only one test and obtain useful information. It was a step by step process wherein each test generates more experience and defined with more precision the performance of the installation. These preliminary results were essential to define the boundary conditions and the facility set up of the main test run. This was a 20hs run test studying the facility. It provides information from full load, and part load operational points at quasi-stationary-state and the transient from one operational point to other. In this process, two main types of test were performed on MoNiKa; on one hand, cold run test, and on the other hand, hot run test.

Condition	Type of Test	number	date	Focus of Research
Preliminary	Cold run	1	07.11.2019	Global Configuration – first approach
Preliminary	Cold run	2	25.11.2019	Pumping System
Preliminary	Hot run	1	28.11.2019	Shot - global configurations
Preliminary	Hot run	2	15.01.2020	8hs static at full load - thermal inertia
Main	**Hot run**	**3**	**23.01.2020**	**20hs at 100/70/50 % mass flow**
Verification	Cold run	3	07.02.2020	Fan Power Consumption

Table 4: Calendar and general description of the test performed at MoNiKa

5.1.1 Cold run

This is the name used to define the test, where the water cycle is not considered. The burner and the pump of the thermal water are turned off, while the ORC cycle is working. This was the first approach that I had with MoNiKa. This test was significant because it helps me to get a good understanding of the facility, to recognize the elements involved, the sensors and components. And to get used to the SIEMENS CONTROL SOFTWARE.

In this type of tests, the analysis in the set up the facility in bypass configuration obtain information to check that all the systems are working correctly, get information from the pumping system, speed and power consumption of the motors (pumps and condenser's fans), and verification of the measurement sensors.

5.1.2 Hot run

In this test, the power plant was fully operating at bypass configuration. The thermal water cycle was working, and the burner was turned on in order to simulate the thermal source. In these tests, the focus was put on the behaviour of the ORC cycle. As boundary conditions, the thermal water temperature was projected to be fixed, and the condenser's fans were fixed at maximum velocity. This last condition was imposed because the temperature control system of the condenser was not working as it should. This malfunction generates a random oscillation of temperature at the condenser outlet.

The goal of this test was to check the whole behaviour of the facility. The main things to determine were: the thermal inertia of MoNiKa, and the thermodynamic values of the organic fluid at different points of the cycle. From them calculate global parameters of the cycle and obtain the inputs to run GESI simulations.

5.2 Preliminary test results

The preliminary tests study MoNiKa's setup. They show the limitations of the facility. These results will define the boundary conditions for the other test and will contribute to build the *knowhow* of MoNiKa.

5.2.1 Sensors reliability and analysis of the Rankine cycle

The first step of the research was to study the reliability of the measurement equipment. In *Chapter 4,* the accuracy of the measurements was discussed. But the first step was to control the measurements and verify, if they are correctly calibrated, or if there was a fail in some of them. This analysis does not have the aim to define a correction factor in order to improve the measurements. The goal is to check and understand why some sensors have differences in its measurements and get a better comprehension of the ORC cycle.

The sensors are installed directly inside the ORC pipe system; it means that it is not possible to extract them to run a calibration test. Under this limitation, it was defined a point in the pipe system where the lectures are trustworthy, and from this point check the rest of the sensors.

The process involves a whole study of the pipe system, studying the pressures and heat losses from one point to the other. The theoretical background applied (energy balance equation and correlations) was discussed in *Chapter 3*. Although this study started at the beginning of the research, only with the results of the preliminary test: Hot Run 1, the entire installation was checked.

5.2.1.1 Point [2] ORC

The initial point was set after the main pump. There are 3 pairs of sensors (temperature and pressure) installed at the same point, and the deviation in the measurement between them were inside the expected accuracy. This condition is not enough to define terms of accuracy and deviation. At this point, the mass flow and density sensor are installed there too. That provides another thermodynamic value of the working fluid to compare with REFPROP to check the measurements.

5.2.1.2 Point [3a] and [3b] ORC

From the pressure measures at the exit of the main pump, the sensor at the exit of the heat exchanger and the ones that are at the entrance of the throttling valve were verified.

In theory, these points are the same, but in MoNiKa we find an isolated pipe from the exit of the heat exchanger to the entrance of the throttling valve, with a height difference of 2m between them. In this case, we find one pair of sensors at the ends of the pipe. As the pipe is isolated, the heat loses are neglected. And the pressure loss plus the difference of height show to fit the measurement's differences.

5.2.1.3 Point [1] [1a] and [1b] ORC

Again, in theory, these three points are the same. However, in MoNiKa, we find another situation. Between the exit of the condenser and the inlet of the main pump, there are 30 meters of uninsulated pipe. We find differences in height between the components. It should also be considered that, at propane tank, the working fluid changes from subcooled to saturated. And finally, the work done by the support pump.

The sensors in the propane tank [1a] were selected as reliable, and from them, the other points were checked. Once the installation is in stationary operation, the mass flow in/out the propane tank is the same and constant, and the level of fluid inside the tank is well defined. This is a free surface at saturation pressure and temperature. The measures in the tank were very good. The comparison of these measurements with REFPROP shows that the nominal value of pressure and temperature measured were almost the same calculated by the software, the deviation of them were less than the expected accuracy. From this point, it was possible to check the measurements of the other two points.

Also, it was possible to determine the heat losses in the pipes. One critical point to study was the temperature of the fluid at the inlet of the main pump [1b]. The study shows that the values of in the sensors are right. The fluid is subcooled.

5.2.1.4 Point [4] ORC

By design, the point [4] is located inside the saturation curve, that's means that the pressure and temperature measures do not define it. To determine this point, we need to find the intersection of the pressure/temperature and quality. In practice, however, the quality at this point cannot be measured. Therefore, this point could not be determined. In the best case, it can be estimated.

Under the assumption that the throttling process is an adiabatic process, no work is done, and the enthalpy of the fluid at the inlet is the same of the fluid at the outlet. The enthalpy calculated at the point [3] is used to intersect with the measurement of the sensors at point [4]. As part of the study, the pressure and heat losses between the outlet of the throttling valve and the entrance of the condenser were estimated. They revealed to be insignificant. Therefore, they were neglected.

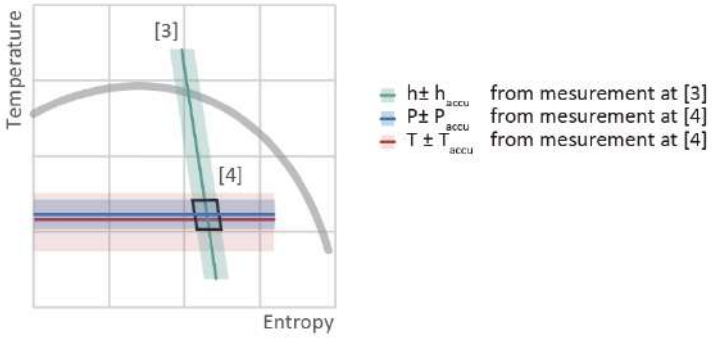

Figure 13: Point [4] estimation

In this case, the accuracy of the pressure sensor installed at point [4] is not better than the accuracy of the temperature sensor. So, both measurements are used for a first delimitation of the maximum deviation possible. In a second step, the enthalpy from the measurements in point [3] and its uncertainty is combined to finally determine the possible maximum and minimum deviation of enthalpy, pressure, and temperature. Using these deviations, the nominal value for this point is calculated.

5.2.1.5 Sensors conclusions

However, as the measurement system is redundant, this cannot provide a better accuracy of the measurements. Al the sensors are calibrated against the same reference. Then the measurement accuracy is not reduced by increasing the number of sensors.

Only in a theoretical context, where all the sensors represent independent measurements and assuming that their calibration is perfect, only in this case, averaging multiple measurements can improve the closeness of the composite measurement to the true value.

From the analysis of reliability and the types of errors present in the measurement, we can conclude that the measurements are trusty, and in all the cases the random error is two orders of magnitude smaller compared with the systematic error. Therefore, in this study, the random errors are neglected, and only the accuracy of the measurement is considered to define and propagate the error. As a result, the accuracy of the measurements is limited to 3 significant digits.

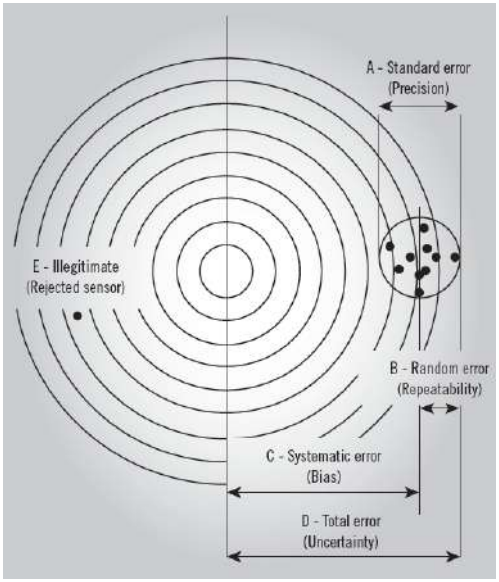

Figure 14: "shooting target". Representation of measures deviations. The center of the target recrements the true value of the measurement. [24]

In relative terms, the data measure in MoNiKa has high precision but low accuracy. The only approach that can be made in order to increase the accuracy is to calibrate the sensors or apply a correction factor, but that is out of the possibilities in this work.

5.2.2 Pumping system analysis

The pump is a key component in the ORC. Its' behavior has a direct impact in the net power generated. The analysis carried out on the pumping system had two objectives: firstly, to define the speeds for different mass flows in order to study part load operations. Secondly, to optimize the efficiency of the set. MoNiKa has the peculiarity of having two pumps in series. This configuration is due to the fact that, it was detected that cavitation could appear at the inlet of the main pump. Therefore, the support pump was added to provide the main one with a pressure of 0.05 MPa above the saturation pressure of the fluid.

ORC Requirement			**Main pump**				**Support pump**				**η tot sys**
pressure	mass flow rate		motor speed	motor power	hyd power	η tot	motor speed	motor power	hyd power	η tot	
MPa	*kg/s*	*%*	*rpm*	*kW*	*kW*	*%*	*rpm*	*kW*	*kW*	*%*	*%*
5,5	3.22	1.12	1442	32.1	30.7	0.96	2161	1.22	0.36	0.30	0.93
	2.9	**1**	**1300**	**27.5**	**26.4**	**0.96**	**2050**	**1**	**0.3**	**0.30**	**0.94**
	2.03	0.7	925	20.0	18.8	0.94	1620	0.63	0.2	0.32	0.93
	1.45	0.5	650	13.9	12.9	0.93	1450	0.48	0.14	0.29	0.91
5	3.25	1.13	1442	28.1	27.2	0.97	2161	1.23	0.32	0.26	0.94
	2.88	1.00	1277	28.4	24.5	0.86	1970	0.98	0.30	0.31	0.85
	2.01	0.70	892	19.9	17.1	0.86	1587	0.60	0.20	0.34	0.85
4.5	3.25	1.13	1442	25.5	24.2	0.95	2161	1.22	0.33	0.27	0.92
	2.88	1.00	1268	26.0	21.8	0.84	1970	0.98	0.30	0.31	0.82
	2.01	0.70	883	18.0	15.3	0.85	1587	0.59	0.20	0.34	0.83
	1.43	0.50	626	12.6	10.9	0.86	1394	0.42	0.14	0.33	0.85

Table 5: pumping system results

At the beginning of this work, there was no relevant information on the main pump. The study then focused on investigating its behavior. Using the sensors installed in MoNiKa was possible to reconstruct the head pressure, mass flow, power consumption, efficiency and speed curves. In the case of the support pump, the necessary information was obtained from the manufacturer [26].

The results show in the *Table 5* correspond to the cold run 1-2-3 (07.11.2019 - 25.11.2019 - 07.02.2020) and they were verified at the hot runs. In the range of temperature of the working fluid at the main pump inlet, (from 5 to 25 C) the deviation of speed is in the range of 2% .While the accuracy of the measurements of power consumption are $\pm 0.2\ kW$ for the main pump and $\pm 0.02\ kW$ for the support pump.

The total efficiency is defined as:

$$\eta_{\,tot\ pump} = \frac{P_{\,hyd}}{P_{EL\ pump}} \qquad (5.1)$$

Where $P_{EL\,pump}$ is the electrical power consumption of the pump and $P_{\,hyd}$ is the hydraulic power delivered to the fluid. This efficiency contempt all the losses in the machine.

The study reveals that the support pump is not working in its optimum point, in some cases a better efficiency can be achieved (in the range of 60%). However, the intention of increasing the efficiency of the support pump has a negative effect on the overall efficiency of both pumps.

The total efficiency of the pumping system is defined as:

$$\eta_{\,tot\ pump\ sys} = \frac{P_{\,hyd\ tot}}{P_{\,EL\ tot}} \qquad (5.2)$$

5.2.3 Mass flow rate conditioning

In the preliminary tests, the pumping system of the ORC and the thermal water cycle were assessed. In these tests, a limitation by the pumps to achieve small values of mass flow was detected. This conditioned directly the possible points of part load.

The analysis of the ORC's pumping system shows that the main pump cannot reach values less than 30 % of $\dot{m}_{ORC\ ds}$. In a second step of the research during the first hot run test (28.11.2019), the thermal water cycle was tested. In this case a second limitation was found, the pump of the water cycle is not able to handle flow rates more than 50% of $\dot{m}_{tw\ ds}$.

Under these conditions and analyses, the equation that describes Q_{trans} in the heat exchanger (*3.13*) with fixed values of temperature of both fluids corresponds to a linear relationship between the two mass flows. This will limit the selection of part loads points, since the minimum possible value of mass flow for setting the facility is $50\%\ \dot{m}_{\,ds}$.

5.2.4 Quasi-steady state conditioning

The second significant limitation is the thermal inertia of the installation. Thermal inertia was underestimated in the first hot run, and actually, it was necessary to perform a specific test to determine the time in which the components reach the thermal equilibrium with the environment (hot run 2 - 15.01.2020). The test revealed that the main pump (LEWA pump) is the component that needs more time to reach the thermal equilibrium.

The first approach was to develop a transient model to describe the thermodynamic behaviour of the pump in time. But the information available was not enough to perform this study, and many factors had to be estimated. This caused this idea to be discarded.

As an alternative, the average temperature of the pump's heads was defined as an indicator of the steady state. The main pump has a temperature sensor (PT100) installed in the oil chamber of each piston (*Figure 15*: Main pump head diagram.).

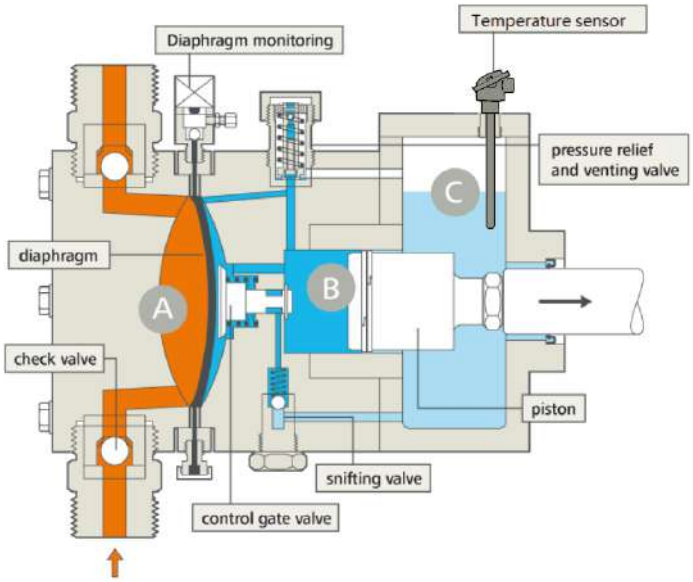

Figure 15: Main pump head diagram. (LEWA M500 triplex)
(A) Working fluid pumper chamber (B) Hydraulic pressure chamber
(C) Oil reservoir for hydraulic fluid (depressurized)

From the analysis of the cold run and the hot run, I found that the temperature at the pump head will rise depending on two factors, the mass flow of the pump and the ambient air temperature. In the case of working at 100% of the mass flow (2.9kg/s), the pump will rise by ~30 K above the ambient temperature, while of 50% of the mass flow (1.45kg/s) the pump will rise by ~20 K above the ambient air temperature (*Figure 16*). Furthermore, an extrapolation of the data indicates that the time to reach 95% of the final temp is 9.5h. and the time to reach the 99% is 11.8h (assuming that the ambient temperature is constant).

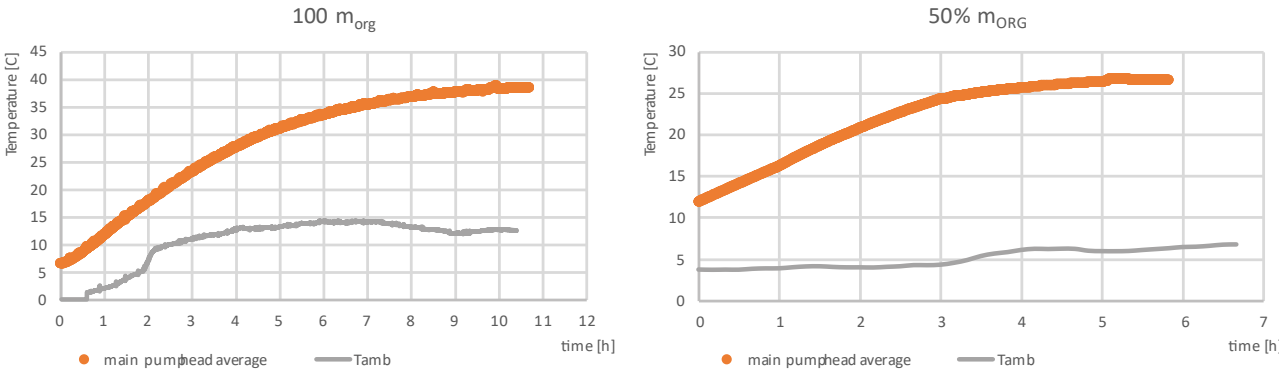

Figure 16: Temperature measurement at the head of the main pump: (*left*) at 100% m_{ORC}. *(right)* at 50% m_{ORC}.

The steady-state regime cannot be achieved in reality. On one hand, the thermal equilibrium depends on the ambient temperature. And on the other hand, the time necessary to perform a stationary study is longer than the time, during which the ambient temperature remains constant.

Under these limitations, a quasi-steady regime is proposed. The condition to achieve this state is defined by a maximum deviation of the average temperature of the main pump's head ≤ 0.5 °C per hour.

$$\frac{\partial \overline{T}_{LEWA\ head}}{\partial t} \leq 0.5 \quad K/h \tag{5.3}$$

This condition is almost at the limit of accuracy that the sensor can measure. The measurements are in the range of 20 to 40 °C; in this range, the calculation of the deviation results in an accuracy of ±0.25 °C.

5.3 Operational loading points selection

At the beginning of the thesis, many points were considered to be used. But due to the limitations of the facility, in particular the long time necessary to reach a thermal equilibrium. These circumstances limit the number of valid operational points to three.

The first one is at full load. It means that the facility will be set to work at its maximum capacity. This point should match with the design point. The other two points are at part load operation. While at full load, MoNiKa is using the 100% of the thermal water mass flow available, a reduced percentage of it is used at part load.

Previous works analysed different configurations possible for part load operation [6], showing special interest in the possibility of working by fixing the ORC pressure and only varying the mass flow. Under this control strategy and keeping a supercritical cycle, I selected the part load conditions at 70% and 50% of $\dot{m}_{ds}$ and at 5.5 MPa of pressure of the working fluid at the inlet of the throttling valve.

5.4 Comparison methodology

In order to compare the results from MoNiKa and GESI, the same approach implemented by Christian Vetter in his PhD work [23] is used. The comparison of the parameters is not only focused on the whole process. They will use as well, to give an analysis of the behaviour of each component.

Parameters

- Rankine cycle points
- Heat exchanged in the Heat Exchanger
- Heat exchanger's fluids temperature in /out
- Heat exchanged in the Condenser
- Power consumption
- ORC mass flow
- Thermal water mass flow
- Quality of the steam after turbine (simulated by an expansion valve)
- Air mass flow invested in the condensation process

It is important to define the way to determinate the accuracy and the deviation between MoNiKa and GESI. Two approach are defined.

- Theoretical results between the experimental data uncertain.
- Definition of a relative deviation

In the first approach, the experimental result from MoNiKa will determinate the validation from GESI results. The comparison will show how good is GESI to predict the behaviour of MoNiKa. In this case, GESI's results show no deviation, and the quality of the simulation is confirmed, if this value is within the experimental uncertainty.

In the second approach, GESI results are weighted, over the experimental data from MoNiKa. The simulations results will be considered as reference. This view, will check how well is the performance of MoNiKa compared to the model.

Absolute error

$$\mathrm{Y} = \mathrm{Y}_{\mathrm{GESI}} - \mathrm{Y}_{\mathrm{MoNiKa}} \tag{5.4}$$

Relative error

$$\Delta\mathrm{Y} = \frac{\mathrm{Y}_{\mathrm{GESI}} - \mathrm{Y}_{\mathrm{MoNiKa}}}{\mathrm{Y}_{\mathrm{GESI}}} \tag{5.5}$$

Both approaches are good models to compare the systems. This work will focus on the comparison using the first approach because it is more appropriate to the aim of this thesis. However, in some cases where the deviations of the measurements cannot be defined, the second approach will be used.

5.5 Final results

5.5.1 Boundary conditions

The results show correspond to the hot run 3 (23.01.2020). This experiment was the result of the previous test performed on MoNiKa during this thesis and will show the current state of the facility.

This previous test defined the information necessary to set the power plant at the required operational points. For example, the protocol for initiating the burner and emulate the hot thermal water source was already tested, as well as the protocol to change from one operational point to the other. At the moment of this work, all the operation was *hand-made*. Furthermore, the pumps' velocity, as well as the percentage of the throttling valve, were defined.

The test was carried out over a period of almost 20 hours. It was necessary to set up three work shifts. The first was led by Dr. D. Kuhn, the second by Gerold Stern, and the last by I. Hans-Joachim Wiemer. The test started on 15.012020 at 6 in the morning. The goal was to reach three operational points in quasi-steady state. The first point at full load (100% mass flow) and the others two at part load. The second point at 70% and the third one at 50% of the design mass flow. (These conditions were discussed in *Chapter 4*).

The weather in this day was particularly stable during the whole test, the variation of the ambient temperature was in the range of 3 °C, which is a good basis for the study since the behaviour of the facility is strongly influenced by this parameter. Another aspect of consideration are the fans of the condenser. They were working at full power during the whole test. Finally, as it was expected to have very low ambient air temperatures, (and in a try to arrive quicker to the thermal equilibrium of the main pump), the container was heated from the day before of the test using a space heater.

5.5.2 Table of results

The *Table 6* list the results obtained in the test performed on 23.01.2020. Here are show the values obtained from the measurements at MoNiKa for the three operational points at quasi-steady state.

	Full Load 100%ṁ	Part Load 70%ṁ	Part Load 50%ṁ	Accuracy	Unit	Location
ORC cycle						
m_{ORC}	2.87	2.03	1.45	±0.03	kg/s	main pump - He Ex.
$T_{AIR\ cond\ out}$	6.79	5.0	3.4	±0.75	°C	chamber Cond, before Fan
T[1]	13.8	10.4	7.3	±0.2	°C	Condenser outlet
p[1]	0.722	0.658	0.602	±0.003	MPa	Condenser outlet
T[1a]	14.3	10.9	7.8	±0.2	°C	propane TANK
p[1a]	0.721	0.655	0.599	±0.003	MPa	propane TANK
T[1b]	14.0	10.6	7.5	±0.2	°C	main pump inlet
p[1b]	0.777	0.710	0.653	±0.003	MPa	main pump inlet
T[2]	17.0	13.3	10.1	±0.2	°C	main pump exit
p[2]	5.53	5.53	5.52	±0.01	MPa	main pump exit
ρ[2]	0.51	0.52	0.52	±0.01	kg/L	main pump - He Ex.
T[3a]	108.1	108.0	107.0	±0.4	°C	He Ex outlet
p[3a]	5.52	5.52	5.51	±0.02	MPa	He Ex outlet
T[3b]	108.3	108.2	107.5	±0.4	°C	Throttling Valve inlet
p[3b]	5.50	5.51	5.50	±0.02	MPa	Throttling Valve inlet
T[4]	14.6	10.9	7.7	±0.2	°C	Condenser inlet
p[4]	0.72	0.66	0.60	±0.01	MPa	Condenser inlet
Water Cycle						
m_{tw}	2.4	1.7	1.2	±0.02	kg/s	-
ρ_{tw}	0.9	0.91	0.91	±0.01	kg/L	-
$T_{tw\ in}$	150.2	150.4	149.6	±0.5	°C	He Ex inlet
$T_{tw\ out}$	61.74	59.3	56.6	±0.3		He Ex outlet
$P_{tw\ in}$	0.886	0.871	0.864	±0.005	MPa	He Ex inlet
$P_{tw\ out}$	0.82	0.815	0.810	±0.005	MPa	He Ex outlet
Ambient						
T_{amb}	0.98	0.66	0.0	±0.75	°C	at MoNiKa
P_{amb}	0.102	0.101	0.101	±0.01	MPa	at MoNiKa
rel. hum.	80	76.9	80.2	±0.4	%	at MoNiKa
Main pump						
vel	1300.0	924	650	±10	RPM	measured at VDS
P_{hyd}	26	19	13.5	±2	kW	calculated
P_{Elec}	27.5	20.2	13.9	±0.2	kW	measured at VDS
Support pump						
vel	1287	1045	1447	±10	RPM	measured at VDS
P_{hyd}	0.31	0.21	0.15	±0.006	kW	calculated
P_{Elec}	1.06	0.63	0.48	±0.02	kW	measured at VDS
Heat transfer $_{He\ Ex}$	894	655	471	±8	kW	Siemens PLC calculation
Throttling Valve	↓8.7	↓6.53	↓4.85	-	%	Percentage of opening

Table 6: 23.01.2020 test results.

6 Analysis

This chapter will analyse the results obtained in the final test. It will study the behaviour of the power plant in general and each component in particular. Furthermore, from this analysis, the corrections parameters of GESI will be defined.

6.1 Global parameters

6.1.1 ORC cycle

From the measurements of pressure and temperature, and using REFPROP, all the thermodynamic values of the ORC cycle were calculated (*Table 7)*. The point [4] cannot be determined, therefore it has to be estimated as it was discussed in *Chapter 4*.

	ORC points	Temp °C	Accu °C	Pressure MPa	Accu MPa	Enthalpy kJ/kg	Accu kJ/kg	Entropy kJ/kg K	Accu kJ/kg K	Quality -
Full Load 100 % ṁ	[1]	13.8	0.2	0.722	0.003	235	0.4	1.12	0.002	Subcooled
	[2]	17.0	0.2	5.53	0.01	245	0.4	1.13	0.002	Subcooled
	[3]	108.3	0.4	5.51	0.02	557	2	2.04	0.005	Superheated
	[4]	14.6	0.2	0.72	0.01	-	353	-	1.227	-
	[4] estimated*	*14.6*	*-*	*0.72*	*0.01*	*557*	*2*	*2.24*	*0.005*	*0.925*
Part Load 70 % ṁ	[1]	10.4	0.2	0.657	0.003	226	0.4	1.09	0.001	Subcooled
	[2]	13.3	0.2	5.53	0.01	236	0.5	1.09	0.002	Subcooled
	[3]	108.2	0.4	5.51	0.02	556	2	2.04	0.005	Superheated
	[4]	11.0	0.2	0.65	0.01	-	358	-	1.260	-
	[4] estimated*	*11.1*	*-*	*0.65*	*0.01*	*556*	*2*	*2.25*	*0.005*	*0.914*
Part Load 50 % ṁ	[1]	7.25	0.2	0.600	0.003	218	0.4	1.07	0.001	Subcooled
	[2]	10.1	0.2	5.5	0.01	228	0.4	1.07	0.001	Subcooled
	[3]	107.5	0.4	5.5	0.02	551	2	2.03	0.005	Superheated
	[4]	7.7	0.2	0.60	0.01	-	364	-	1.290	-
	[4] estimated*	*7.9*	*-*	*0.60*	*0.01*	*551*	*2*	*2.25*	*0.005*	*0.909*

Table 7: ORC thermodynamic values

6.1.2 Heat power

Table 8 shows the values of heat transferred in the heat exchanger, the heat release from the thermal water and the heat absorbed by the propane. And the heat released to the ambient in the condenser. This values are calculated using the equation *(3.15)* for the propane, and the equation *(3.14)* for the thermal water.

	Full Load (100%m) Heat kW	Accu kW	Part Load (70%m) Heat kW	Accu kW	Part Load (50%m) Heat kW	Accu kW
Heat Exchanger						
$Q_{ORC\ in}$	886	10	646	7	462	4
$Q_{tw\ out}$	-899	6	-655	4	-472	3
Condenser						
$Q_{ORCreleased}$	-922	10	-670	7	-482	5

Table 8: Heat power calculated

6.1.3 Thermal inertia

As it was discussed in the *chapter 5*, the condition to establish the equilibrium of the facility with the ambient is defined by the temperature of the main pump. The *Figure 17 (first)* shows temperature as a function of time; in grey are shown the intervals of time where the measurements took place. The following graphics are extrapolations of the measurement data in order to estimate the final temperature of the pump and verify if the condition for quasi-steady state was reached.

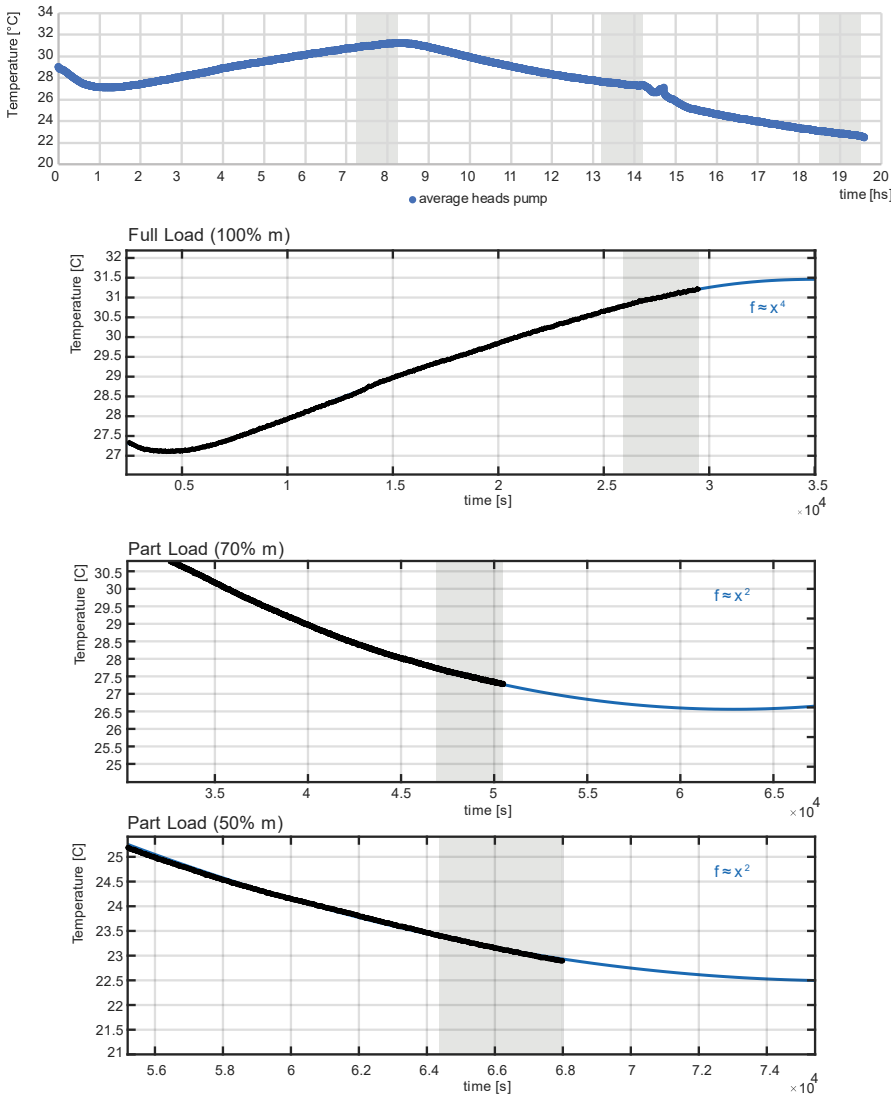

Figure 17: Pump thermal inertia extrapolation.
Black: measure data; Blue matlab extrapolation with polynomial functions

The boundary conditions make that the behaviour of the temperature cannot be projected using a rational function, therefore, polynomic functions were implemented in the fitting. The projections suggest that, since the initial time of recording the measurements until the pump achieves the thermal equilibrium, the deviation is ~1 K. Even though the pre-established condition was fulfilled, the estimations predict a greater deviation than expected. However, this temperature deviation is still not significant for the accuracy that is involve in this work, and will not alter the result of MoNiKa's measurements.

6.2 Component analysis and correction function for GESI

6.2.1 Pumping system and mass flow

The pumping system works as it was projected to be, there are no deviations in the values of pressure or mass flow from the design values, and the system shows to have a very high total efficiency (above the 90% in all the cases). However, it is no possible to calculate the isentropic efficiency, that is needed to use as input for GESI. The sensors do not have enough accuracy to define this value.

	Full Load (100%m)	Part Load (70%m)	Part Load (50%m)
main pump	0.96	0.94	0.97
support pump	0.29	0.33	0.31
pump system	0.94	0.92	0.95
error	0.07	0.07	0.07

Table 9: pumping system total efficiency [%]

To solve this issue, the total pump efficiency is used instead of the isentropic efficiency to run the simulations. The isentropic efficiency is higher than pump efficiency, since this only contemplates losses due to irreversibility in the fluid [27]. Due to the high values of efficiency (*Table 9*), this is a good estimation of the real value of the isentropic efficiency, and in the worst case, it will be a conservative calculation. On the other hand, it has the advantage that GESI can estimate the real power consumption of the pumps [28].

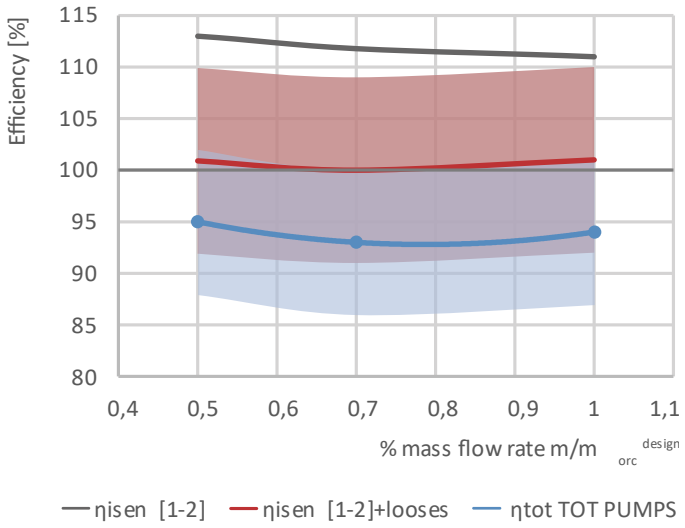

Figure 18: Pumping system efficiency as function of the mass flow

The *Figure 18* shows in black the calculated isentropic efficiency from the outlet of the condenser to the outlet of the main pump. This positive value not realistic. The causes of this results are, in first place the long uninsulated pipes line and the heat losses between both points. The losses of heat affect this value. The red line is a correction of the first one, to estimate a correction factor for the isentropic efficiency, it takes in account the heat losses and the fluctuation from saturated to subcooled that the fluid suffers going through the propane tank. However, in this case, the

assumptions in the correlations and the sensors' accuracy, still propose an unrealistic solution. The blue line corresponds to the total efficiency of the pumping system calculated using the equation *(5.2)*. The areas in colour correspond to the error propagated.

As a result, we can define for further simulations of MoNiKa, the following correlation of the pumping system efficiency as function of the percentage of mass flow rate:

$$\eta_{Pump\ System} = \eta_{AP}\left[1.0933 - 0.42\left(\frac{\dot{m}_{ORC}}{\dot{m}_{ORC\ ds}}\right) + 0.2677\left(\frac{\dot{m}_{ORC}}{\dot{m}_{ORC\ ds}}\right)^2\right] \quad [\%] \qquad (6.1)$$

Where, $\dot{m}_{ORC}$ is the actual ORC mass flow rate that the facility is working, $\dot{m}_{ORC\ ds}$ is the design value, ($2.9\ kg/s$) and η_{AP} is a correction factor for the efficiency (as implemented in GESI for making quickly adaptations).

6.2.2 Heat exchanger

This component shows to have a high heat transfer efficiency, ~98% at the three load cases, with an accuracy of ± 1.5%. This is the result of comparing the heat transferred by the thermal water and the heat absorbed by the propane calculated by the measurement at MoNiKa. Furthermore, the calculation of this value made by the MoNiKa control software turned out to be very accurate.

However, despite this good efficiency, this component does not have the performance expected. The test shows a thermal power of ~900kW at full load configuration with a design value of ~1000kW. (the measured power is 10% less than the projected one). This situation seriously conditions the performance of the whole power plant. Not only the power generation is affected. The major complication is the quality of the fluid after the expansion. When point [4] (condenser inlet) is estimated, I found that the fluid expansion will occur below the design limit for the vapour quality at the turbine outlet of x=0.9.

6.2.2.1 Heat exchanger pressure losses

The value of the pressure losses of the propane and the thermal water can hardly be determined because of the sensors' accuracy. However, the values obtain are in the order of the magnitudes expected.

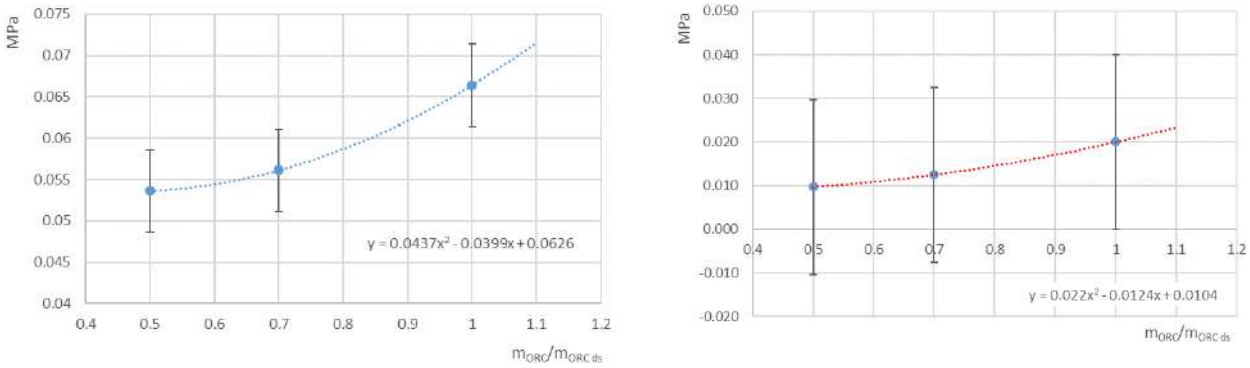

Figure 19: Pressure loses as function of the mass flow in the Heat Exchanger. (*left*) thermal water cycle. (*right*) ORC cycle.

6.2.2.2 Heat exchanger Minimal Temperature Difference (MTD)

The MTD determinates behaviour of the heat exchanger, this parameter has to be strongly modified in order to be adapted in the simulations to the real situation. It was expected to be ~10K, and for the first approach, it was defined at 33.5 K for all the cases. However, there are deviations between the three cases. This difference is expected to happen since each load case is working at different mass flow, and this will change the internal regime in the heat exchanger.

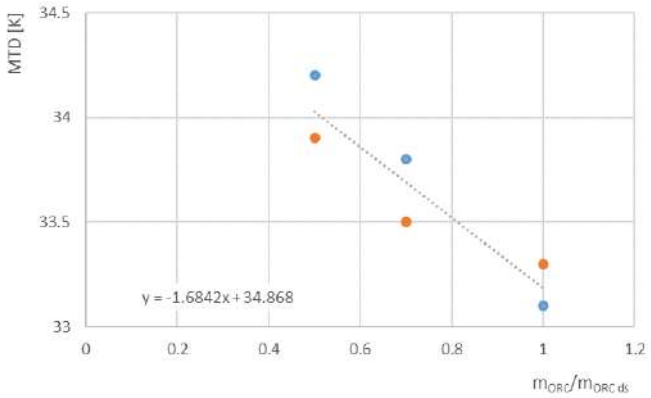

Figure 20: MTD heat exchanger

The MTD coefficient can be optimized to predict the mass flow (blue dots) or to predict the outlet temperature of the thermal water (orange). From both options, a linear interpolation is propose following the previous studies [6] . This approach, equation *(6.2),* shows to be a very good prediction, having a relative error of 0.5% for $T_{tw\ out}$ and 0.1% for relative error for $\dot{m}_{ORC}$.

$$MTD_{He\ Ex} = -1.684\,\dot{m}_{ORC} + 34.868 \qquad [K] \qquad (6.2)$$

6.2.3 Condenser

As the point [4] is only estimated, the study was performed from the air side to check the heat released. Using the air temperature measurement and considering that the fans were working at full power, the heat released was calculated and then the thermodynamic values of the point [4]. The result is not conclusive, although it supports the estimation (the relative error between both approaches is 0.2%), the propagated error from the air side approach for $h_{[4]}$ is 15%.

Although the parameters of the condenser were verified, it was not possible to check the whole behaviour of the condenser. This test was trying to analyse the behaviour of the condenser when it is highly demanded. In throttling operation, it was expected to find superheated steam at the inlet of the condenser. In this scenario, the equipment firstly has to cool the steam and then to condensate it. The simulations suggest that it would be required to release ~1100kW. But in the test, the maximum release heat was of ~930kW.

These results show a behaviour that was not expected. The measurements show that the three cases have almost the same quality (in the subcooled region), and the difference is found in the air temperature at the outlet of the condenser ($T_{\mathrm{AIR\ cond}\ out}$). Although it was expected to find subcooled fluid at the outlet, the presumption was to find differences in the distance from the saturation curve

between the three cases. In particular, in the part load cases since the fans were controlled to work at full power during the whole test.

In the three cases, the fluid at the outlet of the condenser is a little subcooled. This deviation from the theoretical case, where it has to be saturated fluid (x=0) does not impact the results of the simulations. The relative error between the enthalpy and entropy calculated in GESI and the one calculated with the real result from MoNiKa is less than 0.1%

A posterior study determined that the propane tank has a strong influence on the minimal temperature that the condenser can achieve, equation (*6.3*). By setting the mass flow rate, the volume of fluid within the tank is fixed. This fluid is saturated. By lowering the temperature of the inlet fluid, the total mass of propane inside the tank will cool down until it reaches equilibrium with the environment. Once this point is reached, the mass coming from the condenser cannot overcome the thermal inertia of the tank. Otherwise, once the tank achieves its minimum temperature, it will condition the temperature and the quality of the fluid at the outlet of the condenser.

$$T_{cond\ min} = 11.3\ \frac{\dot{m}_{ORC}}{\dot{m}_{ORC\ ds}} + 2.05 + T_{Ambient} \qquad [°C] \qquad (6.3)$$

6.2.3.1 Condenser pressure losses

The pressure of the condenser losses could not be determined; the sensors installed do not have enough accuracy to measure it. To solve this situation, and be able to run simulations in GESI, these values ($\Delta p_{Cond}{}^{*}$) are estimated based on the master thesis of Mariano Fossati [29]. His is studying in deep the condenser transient installed in MoNiKa. From his research, we estimate the pressure losses in the condenser.

	Full Load (100%m)	**Part Load (70%m)**	**Part Load (50%m)**
$\Delta p_{Cond}{}^{*}$	4.42 10^{-3} MPa	2.97 10^{-3} Mpa	2.02 10^{-3} MPa

Table 10: Estimate values for pressure loss in the condenser

The sensors at the inlet of the condenser, point [4], are over a pipe that has a safety function and can be demanded by high pressures. In case that there is a failure in the turbine and while the throttling valve is seating to expand the fluid. A safety piping circuit gets active that protects the condenser, (it connects the propane tank directly with the throttling valve). That is why the model of this sensor has a long operational range (0-10 MPa), and that limits its accuracy.

6.2.3.2 Condenser fan power consumption

As result of this test and the cold run 3 (07.02.2020), a study of the power consumption of the fans was done. Using the information of the manufacturer, the measurement done in MoNiKa and the affinity laws, the equation *(6.4)* was developed. This function calculates the electrical power consumption of the fans as function of the air mass flow, which is defined in turn by the organic mass flow and the temperature of condensation.

$$P_{el\ Fans} = 0.0001028\,\dot{m}_{AIR}{}^{3} - 0.001272\dot{m}_{AIR}{}^{2} + 0.02344\,\dot{m}_{AIR} + 5.309\ [kW] \qquad (6.4)$$

This is a significant step to calculate the real power consumption of the power plan. In a future research, when the study of the turbine is done, they will describe the real Net Power generated.

At the date, this parameter was not fully integrated into the model. Although, the theorical background contemplated this consumption *(3.33),* it just was not estimated.

6.3 Design cycle - Real cycle, comparison

Although the pressure and the mass flow rate are the projected ones for both cycles, the results show that the real cycle presents several deviations from the designed one. It is observed that, the working fluid is not reaching the design temperature at the outlet of the exchanger. This situation has several implications. First, the gross power that MoNiKa can generate is strongly affected. In optimistic simulations, the cycle will generate 26% less energy than what was projected. However, this condition brings another complication. Although point [4] is estimated, it is observed that the isenthalpic expansion of the fluid ends in the two-phase region. This implicates a risk for the turbine operation. In this current situation, under a turbine operation, there are high possibilities that the fluid expands below the quality limit (x=0.9). This implies that the fluid contains liquid droplets and damages the turbine blades.

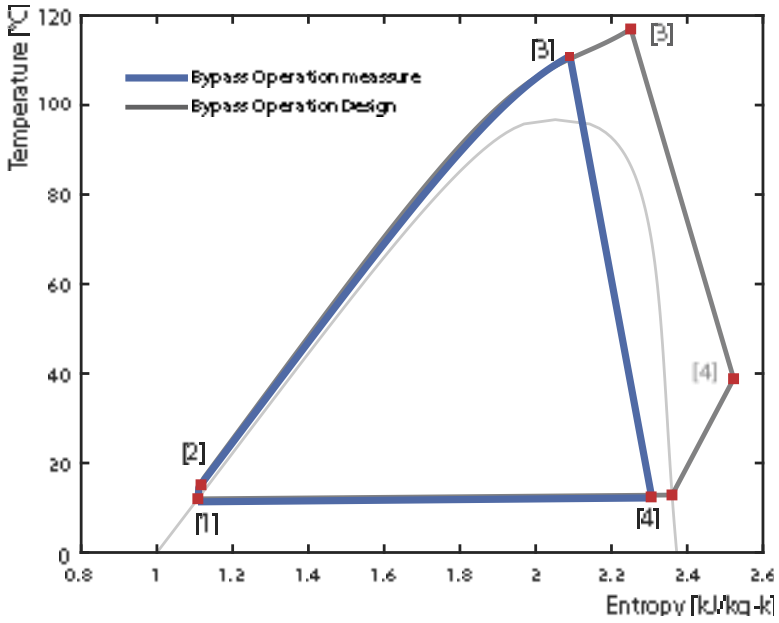

Figure 21: T-s diagram. Comparison between design cycle and measurements at bypass operation

The *Figure 21* shows the comparison between the two cycles in bypass operation. The design cycle is shown in grey and the cycle measured in MoNiKa is shown in blue. The difference is given by the temperature of the live steam vapor at the inlet of the valve, point [3]. This simulation was performed after the test, applying the corrections to the model. Both cases were affected by the same boundary conditions (ambient temperature, pump efficiency and throttling, measured in MoNiKa during final test).

6.4 Power consumption analysis

The equation *(6.4)* together with *(6.1)* conforms the necessary framework to evaluate the power consumptions of the devices installed in MoNiKa as function of the mass flow

Previous research [14] defined that there is an optimum condensation temperature ($T_{cond\ OP}$) where the net power generated is maximum. Increasing the condensation temperature implies a reduction of the gross power *(3.19).* While decreasing this temperature, supposes an excessive consumption of the fans. To analyse this situation, a theorical case is established. With the boundary conditions from the final run, but instead of working in bypass, it is configured in turbine operation (estimating an isentropic efficiency of the turbine = 0.8 for full load case). Although this simulation is a prelaminar approach, where the performance of the turbine is an estimation, and the isentropic efficiency is an optimistic scenario, it reveals the impact of the power consumptions over the net power generation of the power plant.

In this scenario, (*Figure 22*) the analysis reveals that the optimum condensation temperature $T_{cond\ OP} = 12\ °C + T_{Amb}$. It shows that this value will be different for each operational point. Since that, the ORC mass flow (pump and fan consumption), and the turbine efficiency (power generation) will be different in each case.

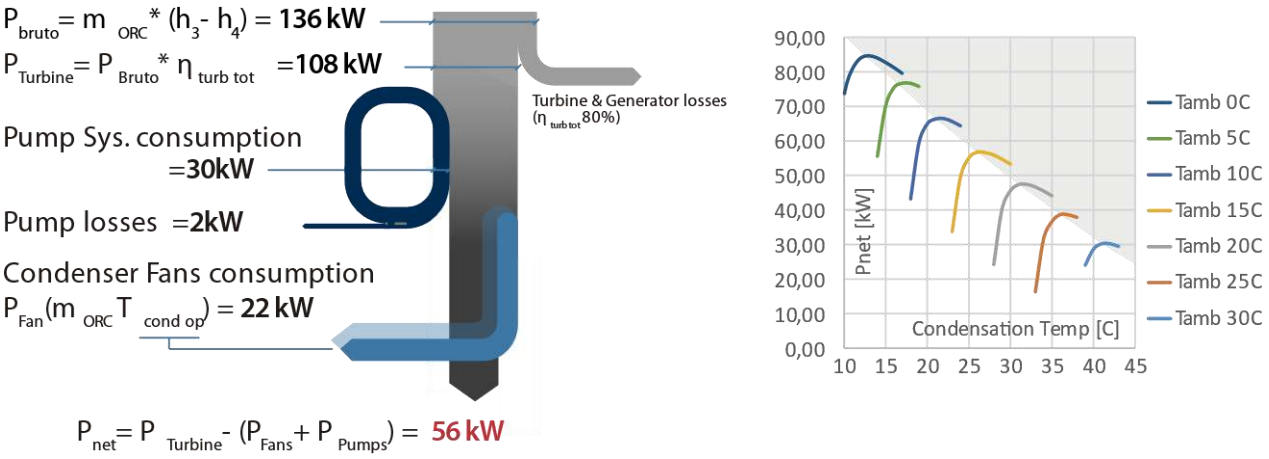

Figure 22: Preliminary simulation for net power optimization
***(left)* Sankey diagram from P_{gross} to P_{net} at MoNiKa**
***(right)* Optimum temperature condensation at MoNiKa's design full load OP**

On one hand, the pump system shows to have an excellent efficiency, therefore the energy that is invest in it, is taken by the working fluid. The losses in the pumping system (2 kW) have a minor impact in the power generation and they do not depend on the condensation temperature. On the other hand, the consumption of the fans can vary from 18 to 60 kW. This represents in the best case, (at $T_{cond\ OP}$), a fan power consumption of 25 % P_{Net}. Away from this optimum temperature, the consumption can reach up to 45% P_{Net}. This scenario exemplifies how critical the fans are and show the strong relationship between them and the performance of the power plant.

6.5 Optimizations

At closing the work, it became necessary to develop a tool that integrates everything investigated in order to have a basis for future research. In this framework, a GESI subprogram was adapted to the current situation of MoNiKa. On the other hand, the situation of the heat exchanger generated a study of possible courses of action to solve the problem.

6.5.1 GESI für MoNiKa

As a result of the investigation, and from the existing structure of the software, a GESI module dedicated exclusively to the MoNiKa's simulation at full-part load was developed. This tool contemplates all the corrections proposed in the previous chapter and automatically adjusts the components' characteristics to the part load situation. The aim is to obtain a most accurate model that can predict different scenarios at MoNiKa for future investigations.

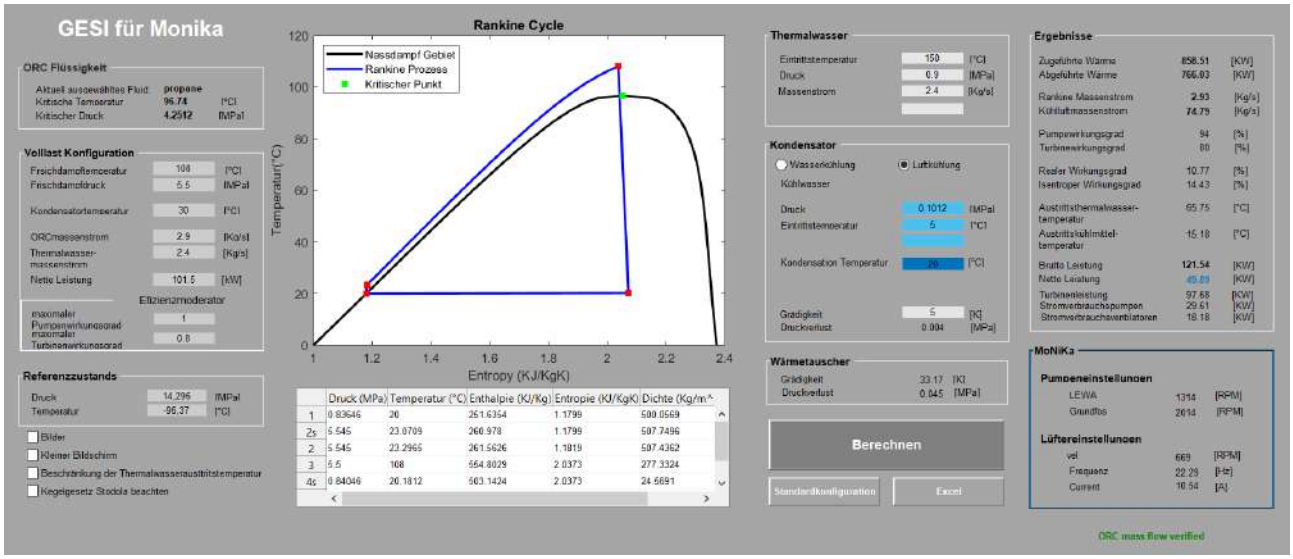

Figure 23: GESI für MoNiKa interface

The interface was redesigned. The first column is reserved to the information of the cycle at its full load operational point; this box is open to futures changes of the parameters. In the middle, the ORC simulation cycle and the ORC points calculation. The second column is reserved for setting the case, the inputs of part load and ambient conditions will define the total scenario. The last column shows all the parameter calculated and it includes a box that estimate the components' settings in MoNiKa.

The module is designed to work without interfering with other systems in GESI, therefore, the main subroutines are not modified. In order to adapt the software, three subroutines are incorporated (*Figure 24*).

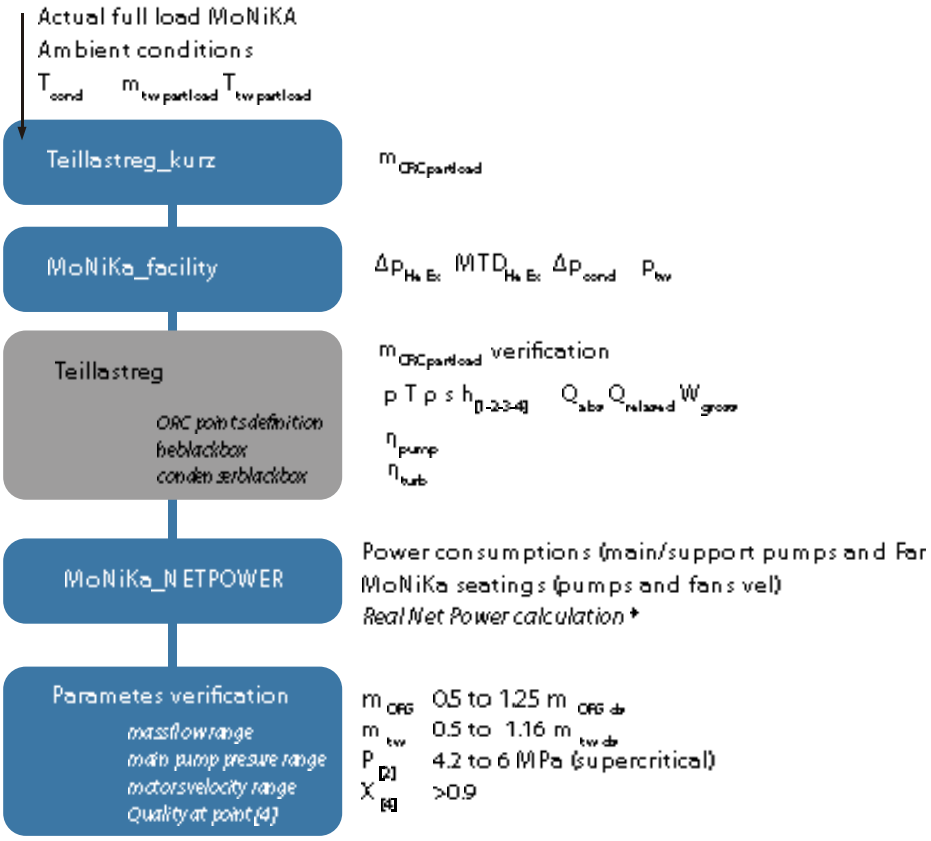

Figure 24: GESI für MoNiKa block diagram

The first step estimates the $\dot{m}_{ORC}$ using the information from the actual state of MoNiKa at full load and the inputs of part load, ambient conditions and condensation temperature. In a second step, the module set the installation characteristics as function of the ORC mass flow. Then the main routine is call, in it all the thermodynamics values are calculated as it was discussed in *Chapter 3*. After that MoNiKa_NETPOWER subroutine is called. The aim of this subroutine is to calculate the real net power generation. Finally, the program checks that the values calculated are in the facility's range. The subroutines are developed in the *Appendix Chapter*.

At the date, the software includes the pumps curves studied at Chapter 5 *as well as the consumption of the condenser's fans. But the turbine behavior is still estimated.*

6.5.2 New full load operational point

The current situation of the heat exchanger implies a re-thinking of the entire cycle looking for a solution that can allow operation with the turbine. Knowing the limitations of the thermal water cycle (where for safety reasons, the TÜV established the maximum parameters at 160°C and 1MPa, and the pump maximum mass flow is 2.8 kg/s). And from the data obtained in the test, different configurations of the ORC and thermal water cycles were simulated on GESI looking for a possible solution.

Mandatory boundary condition: design values from turbine manufacturer

$\eta_{isen\ turb}$ = 0.8 for full load case (design requirement, not verified)

$x_{[4]}$ > 0.9

$\dot{m}_{ORC\ new} \approx \dot{m}_{ORC\ ds}$ (This condition is implemented so that the isentropic efficiency can be estimated as 0.8. For cases with less mass flow, this efficiency is not known, but for sure will be less than this value)

Open parameters:

$T_{[3]}$ free.	$p_{[3]}$ from 4.2 to 6 MPa	$\dot{m}_{ORC}$ ≤ 3.6 kg/s
$T_{tw\ in}$ from 150 to 160°C	$p_{tw\ in}$ ≤ 1MPa	$\dot{m}_{tw}$ ≤ 2.8 kg/s

Under this boundary conditions, three possible scenarios are proposed. The first one considered the thermal water cycle as it was designed, and let free the ORC cycle. This option did not generate any solution since all the options were at ~60% $\dot{m}_{ORC\ ds}$. However, they can be studyied for part load operations.

The second scenario considered fix the ORC cycle and the thermal water temperature to the design values. In this case, the $\dot{m}_{tw}$ has to be 4.7kg/s to fulfil the boundary conditions. It is out of the range of the actual pump, but it opens the option to make a relative cheap investment of equipment. However, the piping system and the heat exchanger have to be study in order to verify if they can work under this mass flow rate.

Finally, the last scenario proposes that both cycles are modified. This generates a very interesting option, where the thermal water is working at its maximum capacity (160°C and 2.8kg/s) and the ORC cycle live steam conditions are: 5.5 MPa and 115°C° in this case, the $\dot{m}_{ORC}$ = 2.7 kg/s (93% $\dot{m}_{ORC\ ds}$), and the quality after the expansion of the propane is 0.92. Furthermore, the estimations of the thermal power are in the range of ~1000kW.

At the date of this work, this is a theorical solution. There was no time due to the closure of the university to perform the test at MoNiKa.

7 Conclusions

In the present work, the MoNiKa cycle in bypass operation at a stationary regime was studied. In order to fulfil this goal, the first step was the study of the sensors installed in the facility and to determine the accuracy of the measurements. Then the operating limits of the plant were studied and established. Finally, a quasi-steady state study was carried out at three operational points, where the behaviour of the entire power plant as well as each component was analysed.

Even though the current situation in MoNiKa presents a great challenge and the current results make us rethinking its design conditions, far from discouraging research, they open the door to continue searching and developing the state of the art of this technology.

The dual condition of the installation, as power plant, but at the same time, as a research platform, exposes the problem of sensors' accuracy. It is very good to measure the behaviour of the facility like a power plant. However, it is not good enough to provide the exactitude needed for research works. The pressure losses of the heat exchanger and the condenser are in the range of the sensors' uncertainty. Furthermore, the measurements at the condenser's inlet cannot define the thermodynamic state of the fluid.

The lectures of pressure and temperature are limited to three significant digits, which is not enough to define the specific entropy or enthalpy. This limitation is reflected at the moment of trying to calculate the isentropic efficiency of the pumps.

The analysis in the components leads to other conclusions. The study of the pumping system shows that it is not possible to increase the efficiency of the set. Although it is possible to improve the total efficiency of the support pump, it will negatively impact on the overall performance of the system. Therefore, the support pump has to be optimised to only provide the main pump with the enough pressure to avoid cavitation at any moment. $\Delta P_{support\ pump}$ = 0.05 Mpa.

The current situation of the heat exchanger makes it necessary to redefine the design point. In this work, a compromise solution is proposed between both cycles (water and ORC):

ORC cycle Live steam conditions 5.5 MPa and 115 °C | $\dot{m}_{ORC}$ = 2.7 kg/s (93%$\dot{m}_{ORC\ ds}$)
tw cycle $T_{tw\ in}$ in = 160 C | $\dot{m}_{tw}$ = 2.8kg/s

This new design for full load operational point is the result of the simulations performed with GESI with the corrections already discussed, and considering the limits of the thermal water cycle.

This is a starting point for futures research, which has to be verified in the plant working at bypass configuration. If it is possible to achieve, it will allow the next stages of investigation to be followed without the need for investment in new equipment. It is mandatory to define a new full load operational point that allows working in turbine operation without risk of damaging the equipment.

The ORC technology by its own nature, of using low enthalpy sources, is strongly influenced by the ambient conditions, specially by the ambient temperature. This condition has a direct influence in the power generation of the power plant, and affects the behaviour of many components (optimum condensation temperature in the condenser, saturation equilibrium in the propane tank and the thermal equilibrium of the pumping system). This factor will determine the viability of a geothermal project.

In terms of optimization the energy production, the analysis showed that the most significant energy consumption occurs in the fans, their performance significantly affects the net power generation. Optimizing this component is essential to achieve the best performance of the power plant. Following with analysis performed in this study, the focus has to be the implementation of the spray in the condenser (wet operation). This configuration may have a significant influence on increasing the net power generation. Furthermore, to define the optimum condensation temperature, a complete analysis of the turbine+generator performance has to be done. An equation similar to (*6.1*) that relates the actual energy delivered to the electrical grid as a function of the mass flow is necessary to be defined.

Finally, we cannot forget in futures analysis the power consumption of the thermal water pump. In this work, this component was neglected and the focus of the research was on the ORC cycle. However, the power consumption of the thermal water pump as well as, the fans and the propane pumps have to be taken in consideration to define the net power generated by the power plant.

8 Bibliography

[1] Klein, D. R.; Carazo, M. P.; Doelle, M. et al.: The Paris agreement on climate change. Analysis and commentary / edited by Daniel Klein, María Pía Carazo, Meinhard Doelle, Jane Bulmer, and Andrew Higham. Oxford: Oxford University Press 2017

[2] DiPippo, R.: Geothermal power plants. Principles, applications, case studies and environmental impact / Ronald DiPippo. Amsterdam: Butterworth-Heinemann 2015

[3] A. Rettig, M. Lagler, T. Lamare, S. Li, V. Mahadea, S. McCallion, J. Chernushevich: Application of Organic Rankine Cycles (ORC). Word Engineers' Convention. 4-9 september 2011

[4] Christian Vetter, Hans-Joachim Wiemer and Dietmar Kuhn: Comparison of sub- and supercritical Organic Rankine Cycles for power generation from low-temperature/low-enthalpy geothermal wells, considering specific net power output and efficiency. Applied Thermal Engineering 51 (2013) 1-2, S. 871–879

[5] Kuhn, D. (2.) (M.): Modular Low Temperature Cycle Karlsruhe. Internet: www.monika.kit.edu/english

[6] Vetter, C.; Wiemer, H.-J.; Kuhn, D.: Comparison of sub- and supercritical Organic Rankine Cycles for power generation from low-temperature/low-enthalpy geothermal wells, considering specific net power output and efficiency. Applied Thermal Engineering 51 (2013) 1-2, S. 871–879

[7] National Centers for Environmental Information. Stand: 10.10.2019. Internet: https://www.ncdc.noaa.gov/. Zugriff am 1010/2019

[8] Wiemer, H.-J.: general conversations with thesis coordinator. KIT campus north - ITES 2019 winter semester. e-mail: wiemer@kit.edu

[9] ITES: Documentation about Monika design process and development. ITES internal server IKET-NAS-03/geothemie/MoNiKa

[10] Bejan, A.: Advanced engineering thermodynamics. Hoboken, New Jersey: John Wiley & Sons (2016)

[11] ITES Institute for Thermal Energy Technology and Safety: GESI. Geothermal Simulation. 2018

[12] REFPROP. Reference Fluid Thermodynamic and Transport Properties Database. NIST National Institute of Standards and Technology (2018)

[13] Vetter, C.: Thermodynamische Auslegung und transiente Simulation eines überkritischen Organic Rankine Cycles für einen leistungsoptimierten Betrieb. Karlsruhe: KIT Scientific Publishing (2014)

[14] Christian Vetter, H. Joachim Wiemer: Dynamic Simulation of a Supercritical ORC using Low-Temperature Geothermal Heat. Melbourne, Australia (2015)

[15] Çengel, Y. A.; Boles, M. A.: Termodinámica. México [etc.]: McGraw Hill (2015)

[16] Çengel, Y. A.; Cimbala, J. M.; Turner, R. H.: Fundamentals of thermal-fluid sciences. New York NY: McGraw-Hill Education (2017)

[17] PROFIBUS & PROFINET International. Stand: 08.02.2020.
Internet: https://www.profibus.com/. Zugriff am 08.02.2020

[18] NIST Pages. Stand: 13.01.2020. Internet: https://pages.nist.gov/REFPROP-docs/. Zugriff am 13.01.2020

[19] Alessio Suman: Uncertainty Quantification of Performance Parameters in a Small Scale ORC Test Rig, (2019)

[20] Randall Manteufel, A. K.: Influence of uncertainties and assessment of significant digits in thermodynamics. Computer Science (2013)

[21] DIN Deutsches Institut für Nornniing e.V: 1319-3. Grundlagen der Meßtechnik

[22] DIN Deutsches Institut für Normung e.V.: 1319-1. Grundlagen der Meßtechnik

[23] Joint Committee for Guides in Metrology: Evaluation of measurement data — Guide to the expression of uncertainty in measurement. JCGM (2010)

[24] Béla Lipták: We need a standard for stating measurement accuracy Level & Flow State of Technology ebook (2016)

[25] Karlsruhe Institute of Technology: Rules for Safeguarding Good Scientific Practice at Karlsruhe Institute of Technology (KIT). November 17, 2014.

[26] Grundfos Pumps Ltd: Grundfos - product center

[27] Arnaud Landelle, Nicolas Tauveron, Rémi Revellin, Philippe Haberschill, Stephane Colasson, et al.: Performance investigation of reciprocating pump running with organic fluid for organic Rankine cycle., Applied Thermal Engineering, Elsevier (2017)

[28] Landelle, A.; Tauveron, N.; Revellin, R. et al.: Performance investigation of reciprocating pump running with organic fluid for organic Rankine cycle. Applied Thermal Engineering 113 (2017), S. 962–969

[29] Mariano Fossati: Simulation and Validation of a transient condenser for a Supercritical Organic Rankine Cycle. Master Thesis, ITES, Karlsruhe Institute of Technology, (2020)

9 Appendix

9.1 MoNiKa's sensors location and pipe diagram

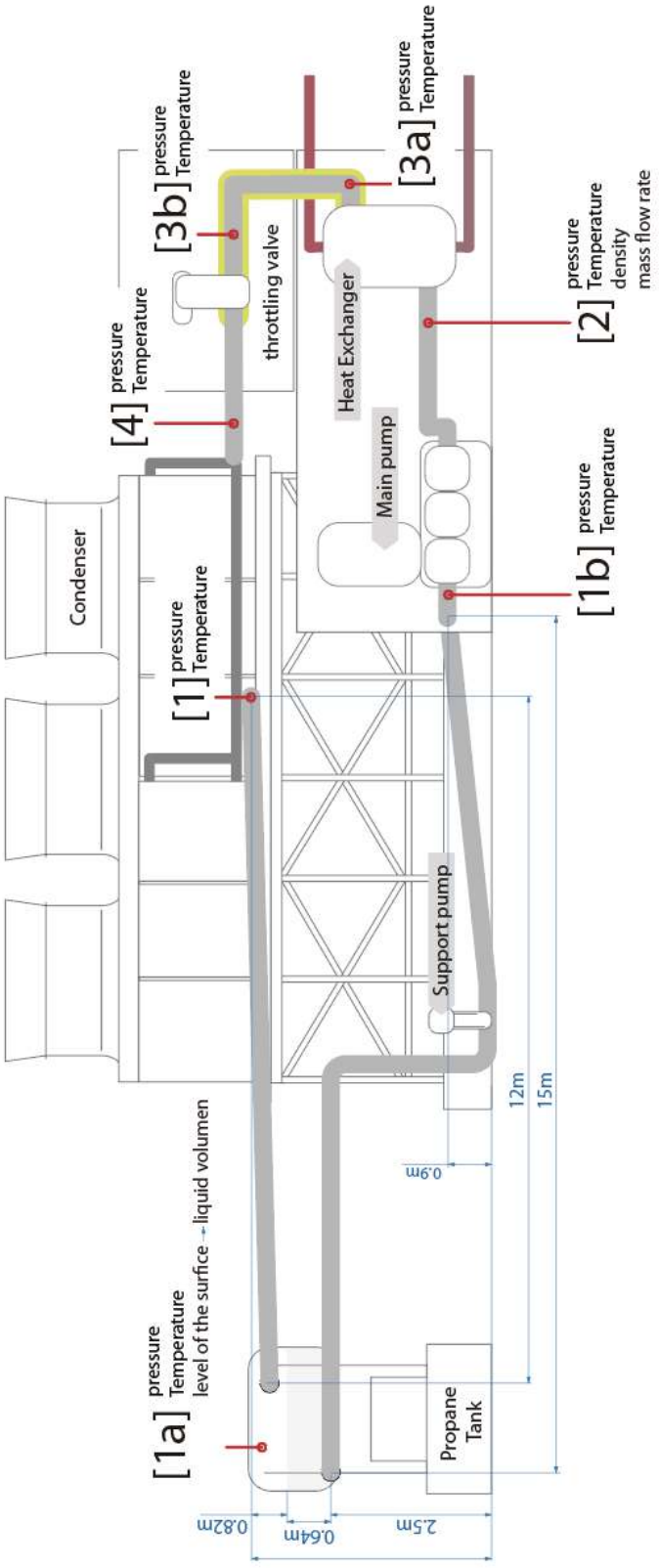

9.2 MoNiKa's component list

List of the components and its descriptions installed in MoNiKa that were used in this work.

main components		Description	Code	Manufacturer	Model	Coment
		ORC support pump	10P1	Grundfos	CRN20-04 E-FGJ-G-E	centrifuge
		ORC main pump	10P2	LEWA	triplex M514US G3G	diaphragm
		Heat exchanger	20W1	Gesmex	-	1000 kW
		Expansion Valve	11PRV01	Vetec	type 73,7	-
		Condenser	40W1	KÜHLTURMKARLSRUHE	KAKVH	air coling fluid
		Propane Tank	10B1	KAH	-	2400L PN25 bar

sensors	Point	Location	Code	Manufacturer	Model	Range
pressure	[1]	Condenser outlet	PS 10-05	VEGA	Vegabar82	-1-25bar
	[1a]	Propane Tank - Pump inlet	PI 10-06	VEGA	Vegabar82	-1-25bar
	[1a]	Propane Tank - Pump inlet	PS 10-06	VEGA	Vegabar82	-1-25bar
	[1b]	Between pumps	PS 10-11	VEGA	Vegabar82	-1-25bar
	[2]	Heat exchanger inlet	PS 10-01	VEGA	Vegabar82	0-100bar
	[2]	Heat exchanger inlet	PI 10-01	VEGA	Vegabar82	-1- 100 bar
	[2]	Heat exchanger inlet	PI 10-09	VEGA	Vegabar82	-1-100 bar
	[3a]	Heat exchanger outlet	PI 10-10	VEGA	Vegabar81	0-100bar
	[3b]	Expansion Valve inlet	PS 10-02	VEGA	Vegabar81	0-100bar
	[3b]	Expansion Valve inlet	PI 10-02	VEGA	Vegabar81	0-100bar
	[4]	Condenser inlet	PS 10-04	VEGA	Vegabar82	-1-100 bar
	[4]	Condenser inlet	PI 10-04	VEGA	Vegabar 82	-1-100bar
	-	tw cycle (He. Ex. inlet)	PI 20-01	VEGA	Vegabar81	-1-25bar
	-	tw cycle (He.ex. outlet)	PI 20-02	VEGA	Vegabar82	-1-25bar
temperature	[1]	Condenser outlet	TS 10-05	WIKA	TR34 class A	PT100 -30 to 250 C
	[1a]	Condenser outlet	TI 10-05	WIKA	TR34 class A	PT100 -30 to 250 C
	[1a]	Propane Tank - Pump inlet	TI 10-06	WIKA	TR34 class A	PT100 -30 to 250 C
	[1b]	Between pumps	TS 10-08	WIKA	TR34 class A	PT100 -30 to 250 C
	[2]	Heat exchanger inlet	TS 10-01	WIKA	TR34 class A	PT100 -30 to 250 C
	[2]	Heat exchanger inlet	TI 10-01	WIKA	TR34 class A	PT100 -30 to 250 C
	[2]	Heat exchanger inlet	TI 10-09	WIKA	TR34 class A	PT100 -30 to 250 C
	[3a]	Heat exchanger outlet	TI 10-10	WIKA	TR34 class A	PT100 -30 to 250 C
	[3b]	Expansion Valve inlet	TI 20-02	WIKA		
	[3b]	Expansion Valve inlet	TI 10-02	WIKA	TR34 class A	PT100 -30 to 250 C
	[4]	Condenser inlet	TI 10-04	WIKA	TR34 class A	PT100 -30 to 250 C
	-	geo cycle	TI 20-01	WIKA		
	-	geo cycle	TS 10-02	WIKA	TR34 class A	PT100 -30 to 250 C
mass flow	[2]	propane cycle	FI 10-01	Promass	83F	
	-	geo cycle	FI 20-01	Promass	83F	
density	[2]	propane cycle	FI 10-01	Promass	83F	
	-	geo cycle	FI 20-01	Promass	83F	

9.3 Full schematic MoNiKa power plant

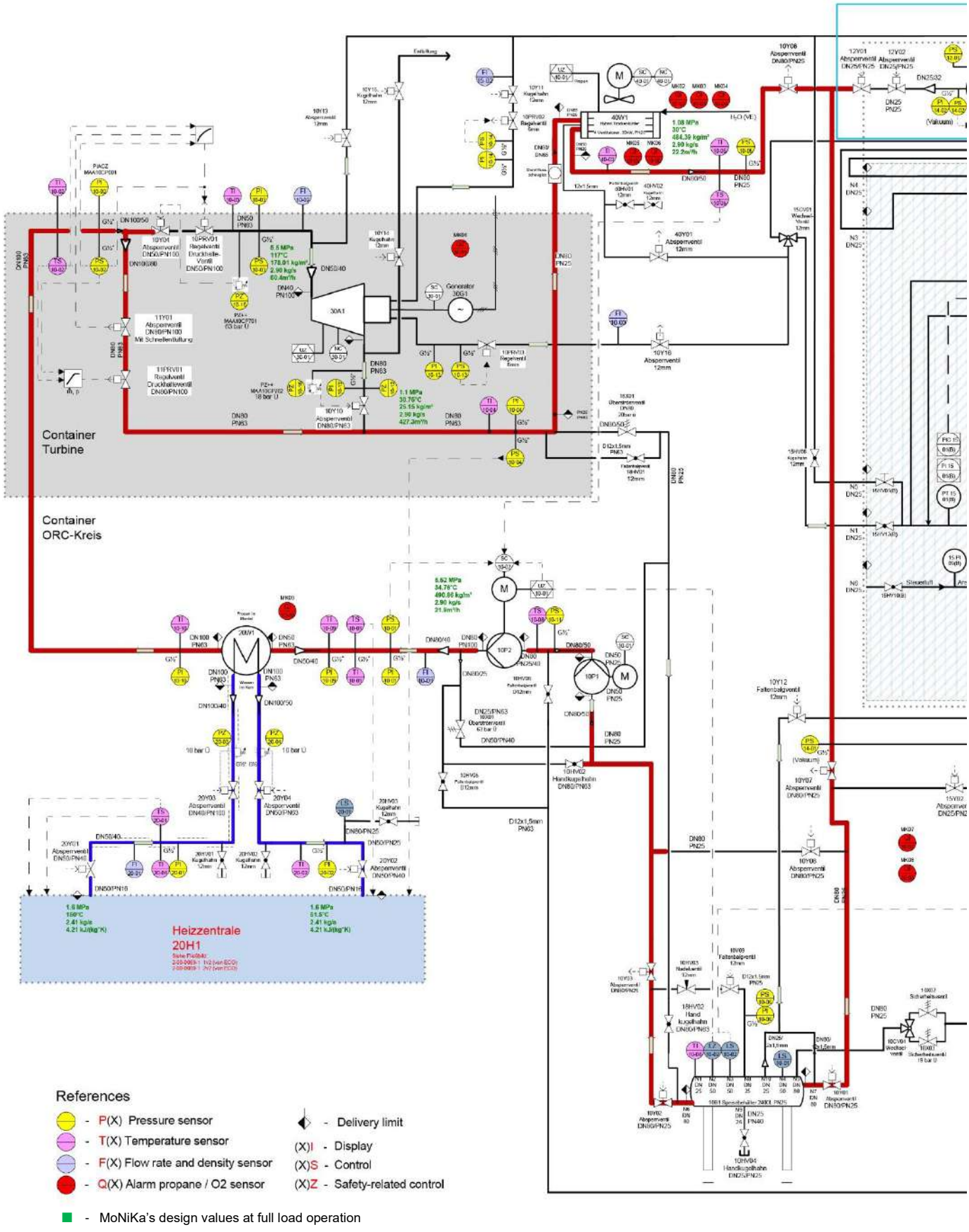

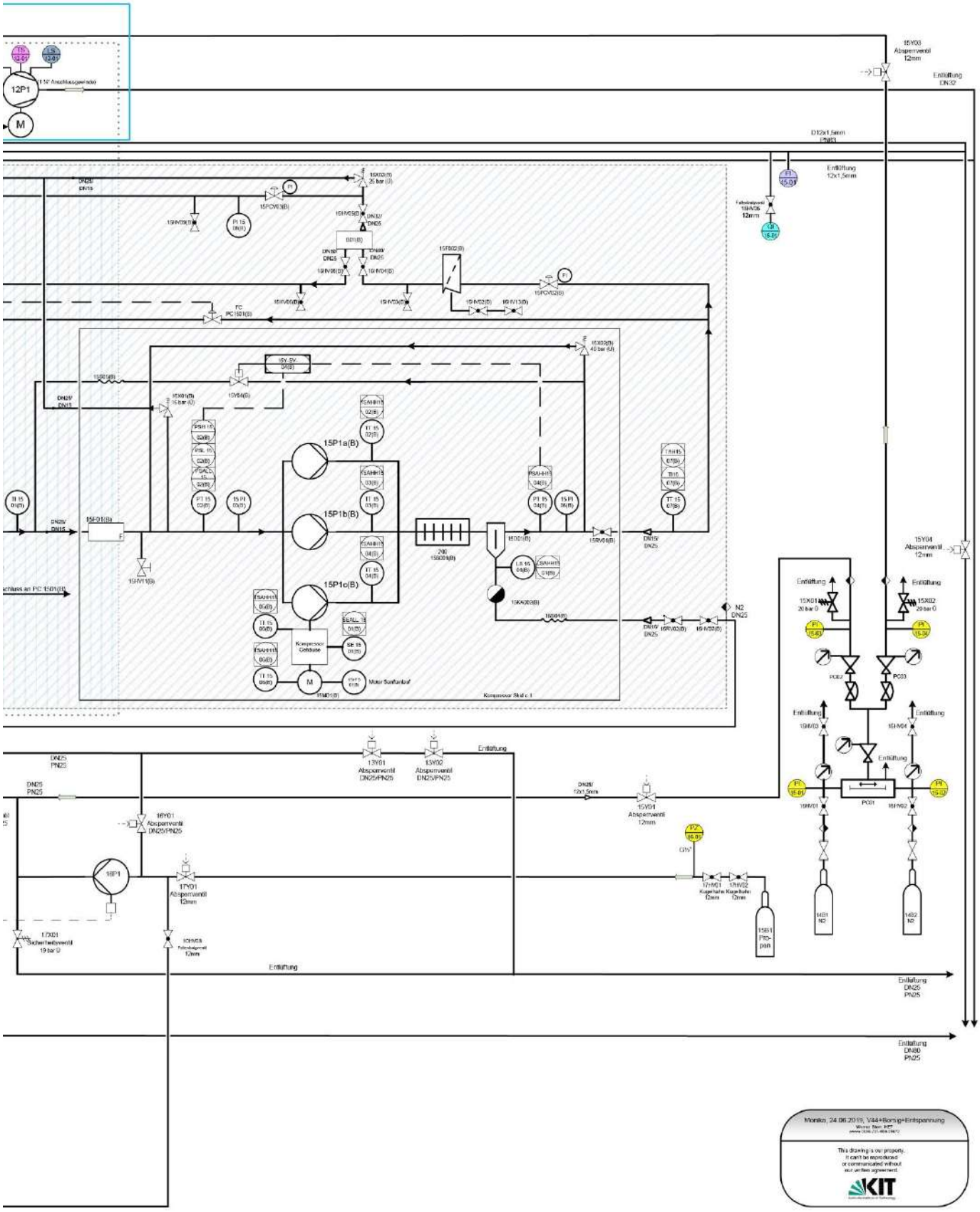
12P1
M
15Y03
Absperrventil
12mm
Entlüftung
DN32
Entlüftung
12x1,5mm
15P1a(B)
15P1b(B)
15P1c(B)
15Y04
Absperrventil
12mm
N2
DN25
Entlüftung
15X01
15X02
PC02
PC03
PC01
13Y01
Absperrventil
DN25/PN25
13Y02
Absperrventil
DN25/PN25
16Y01
Absperrventil
DN25/PN25
16P1
17Y01
Absperrventil
12mm
17X01
Sicherheitsventil
19 bar ü
15Y01
Absperrventil
12mm
Entlüftung
DN25
PN25
Entlüftung
DN80
PN25
Monika, 24.06.2015, V44+Bürsig+Entspannung
This drawing is our property.
It can't be reproduced
or communicated without
our written agreement.
KIT

9.4 Main pump (LEWA) curves

characteristic curves reconstructed for 5.5 MPa (full load design pressure)

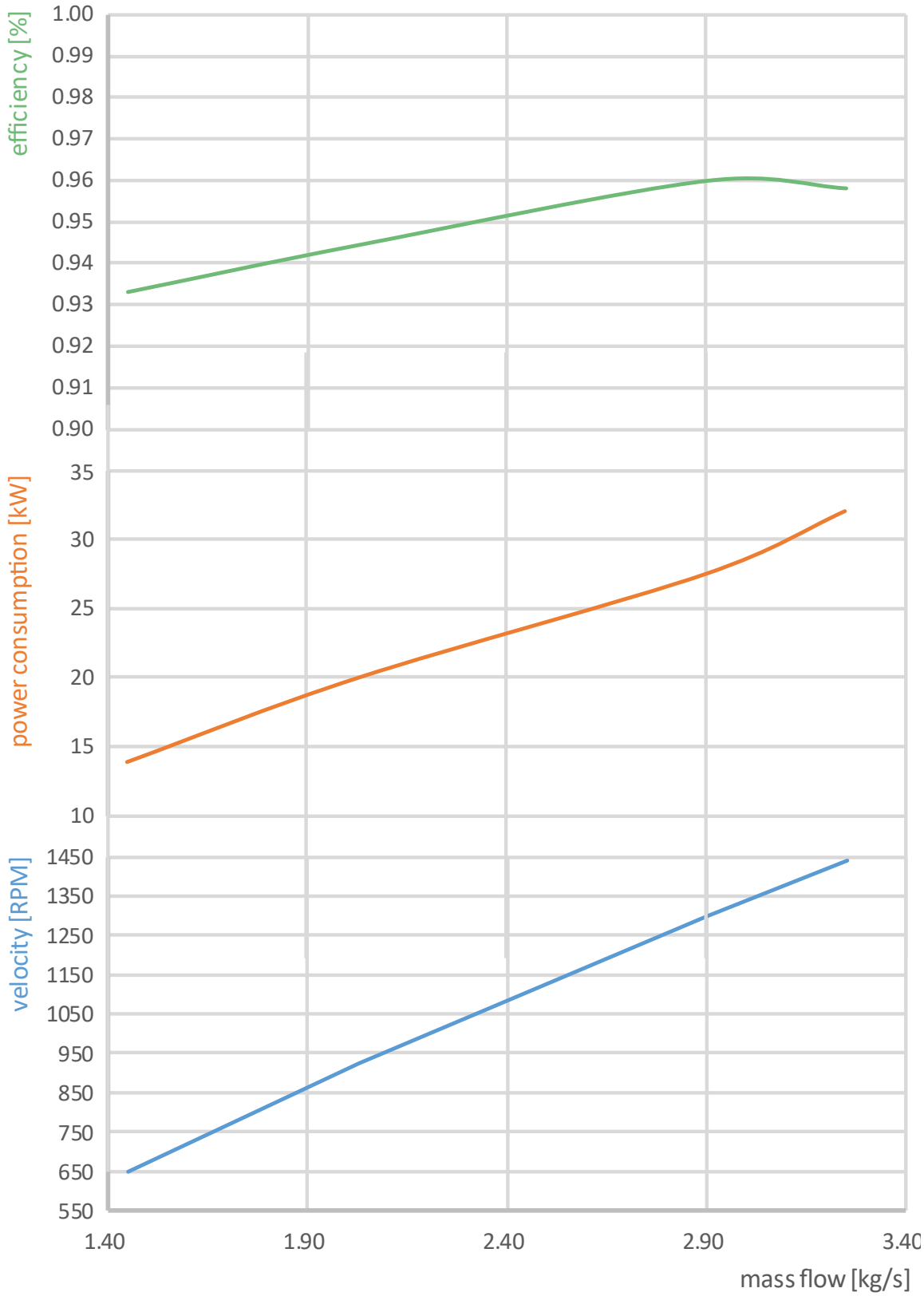

9.5 Main run (23.01.2020) measurement graphics

This section will show the measurements results from the main run performed on MoNiKa for futures studies of the installation in stationary regime or to analyse the transient times of the components.

9.5.1 Main pump temperature curves

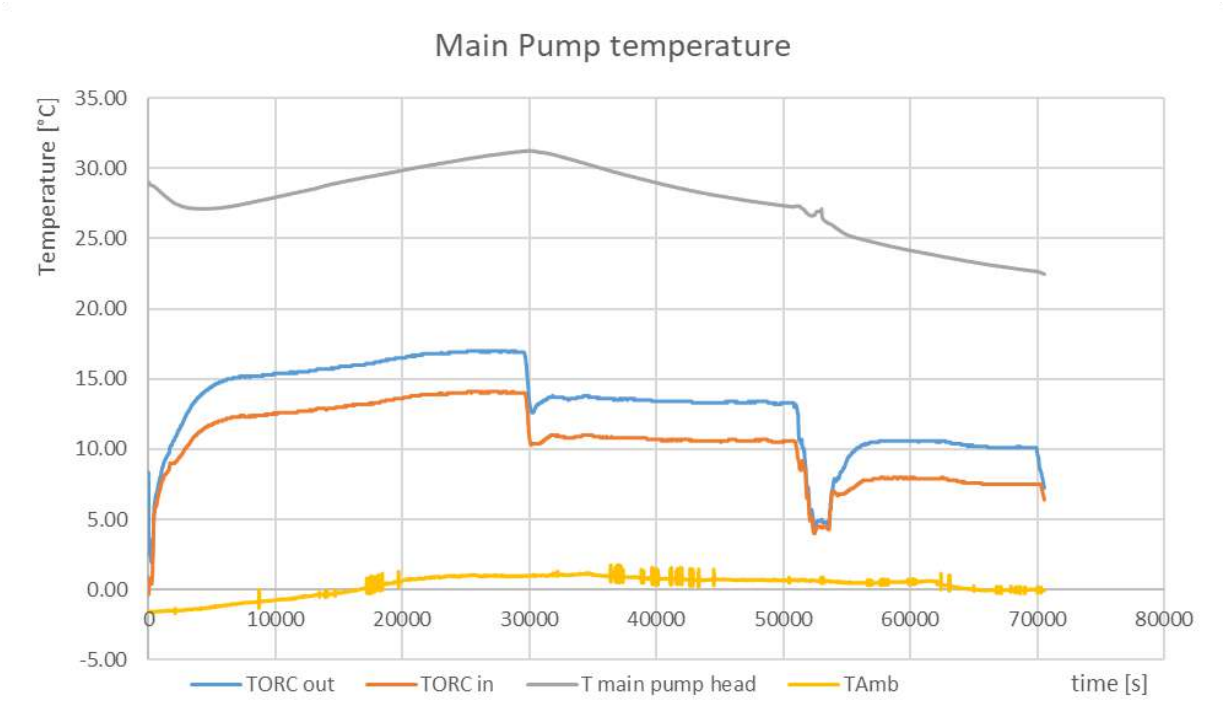

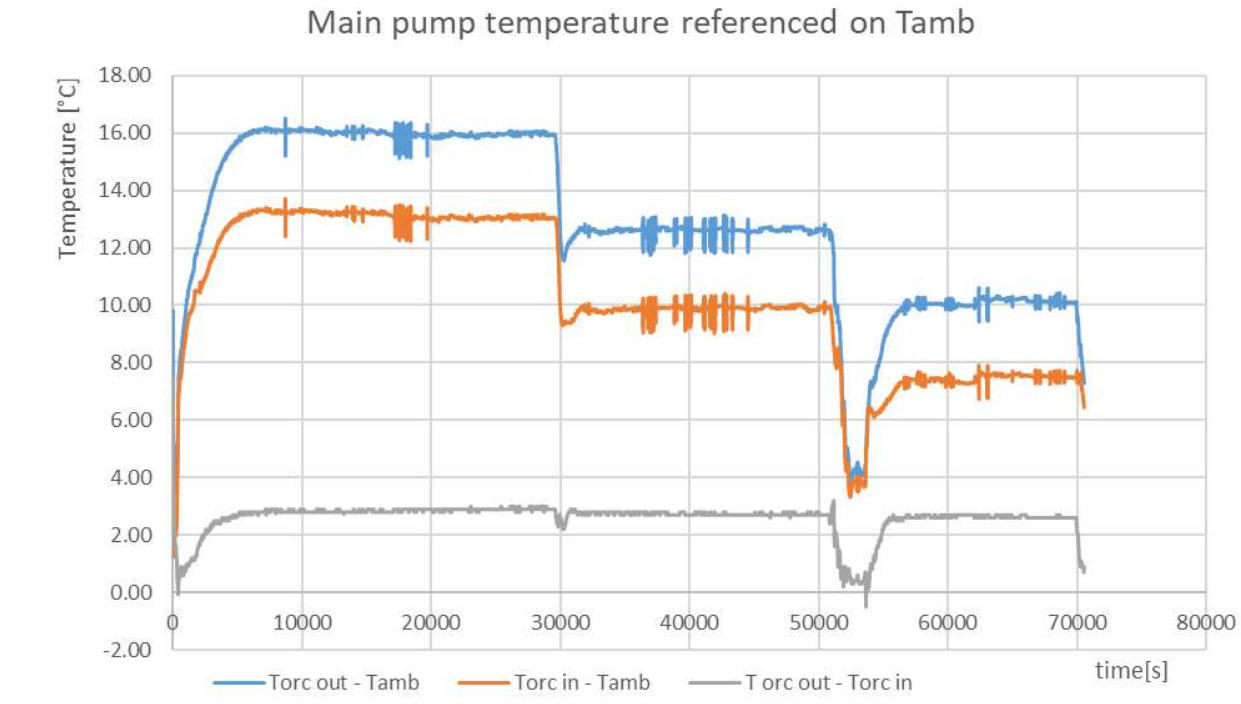

9.5.2 Heat exchanger curves

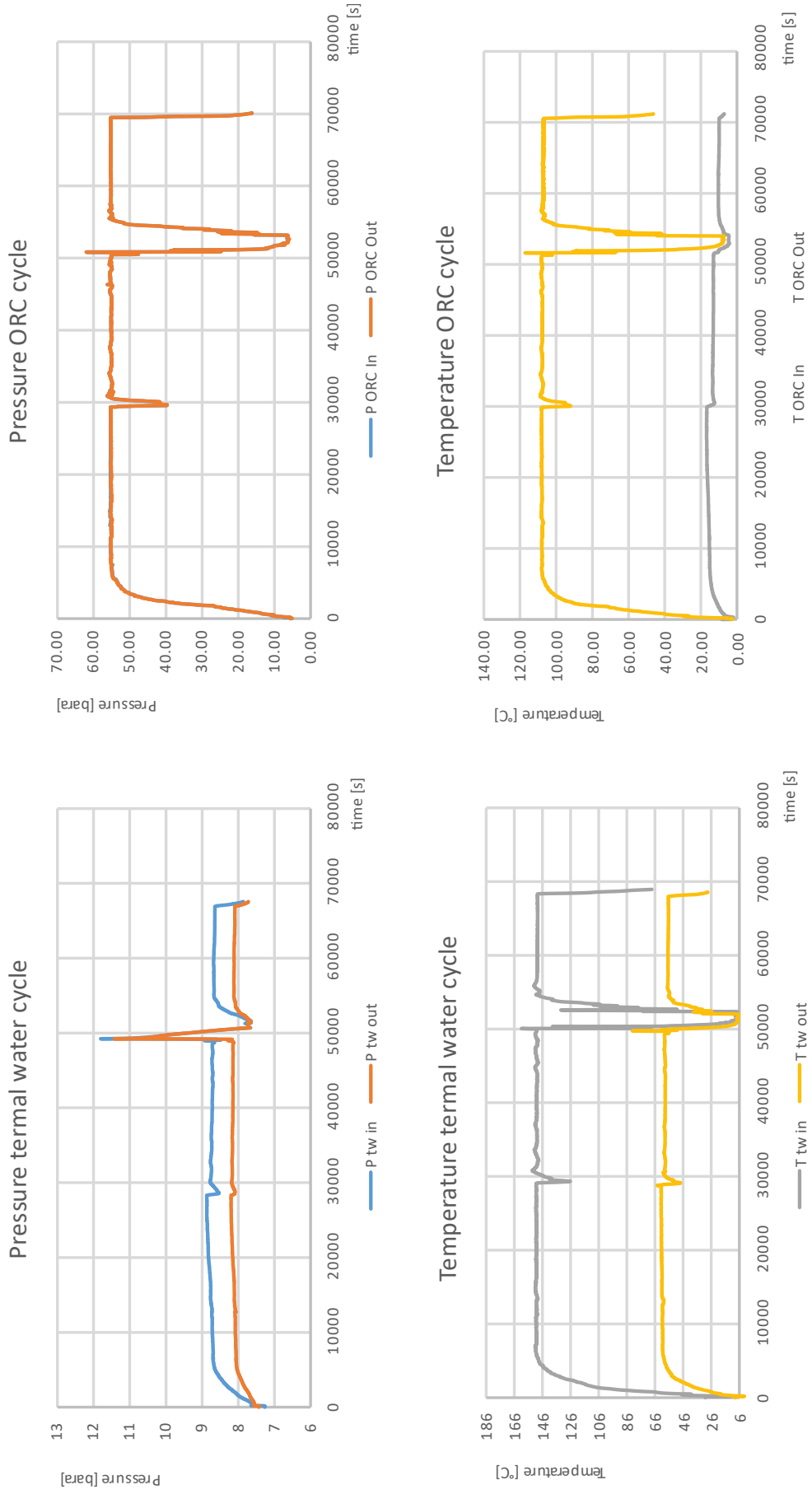

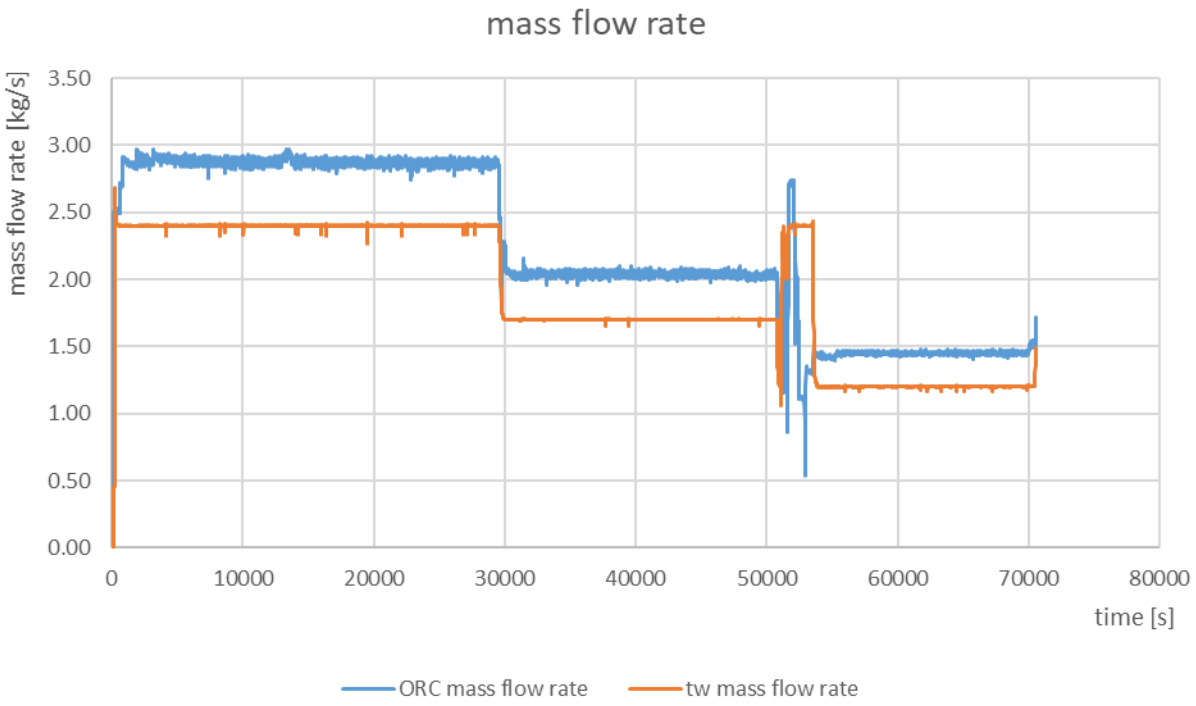
mass flow rate
mass flow rate [kg/s]
3.50
3.00
2.50
2.00
1.50
1.00
0.50
0.00
0
10000
20000
30000
40000
50000
60000
70000
80000
time [s]
ORC mass flow rate
tw mass flow rate

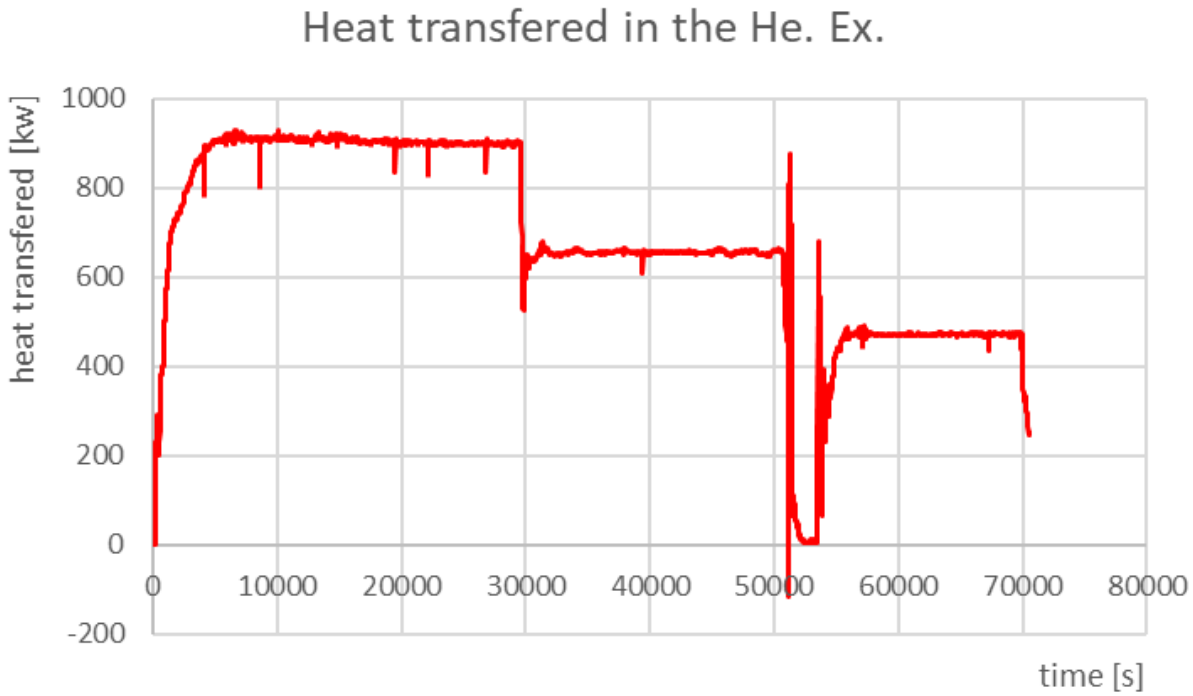
Heat transfered in the He. Ex.
heat transfered [kw]
1000
800
600
400
200
0
-200
0
10000
20000
30000
40000
50000
60000
70000
80000
time [s]

9.5.3 Condenser curves

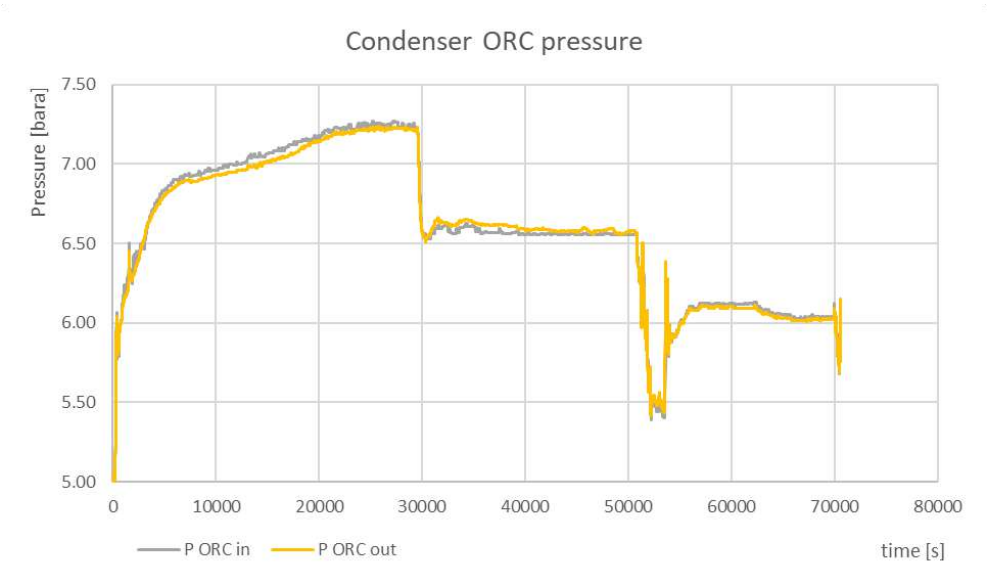

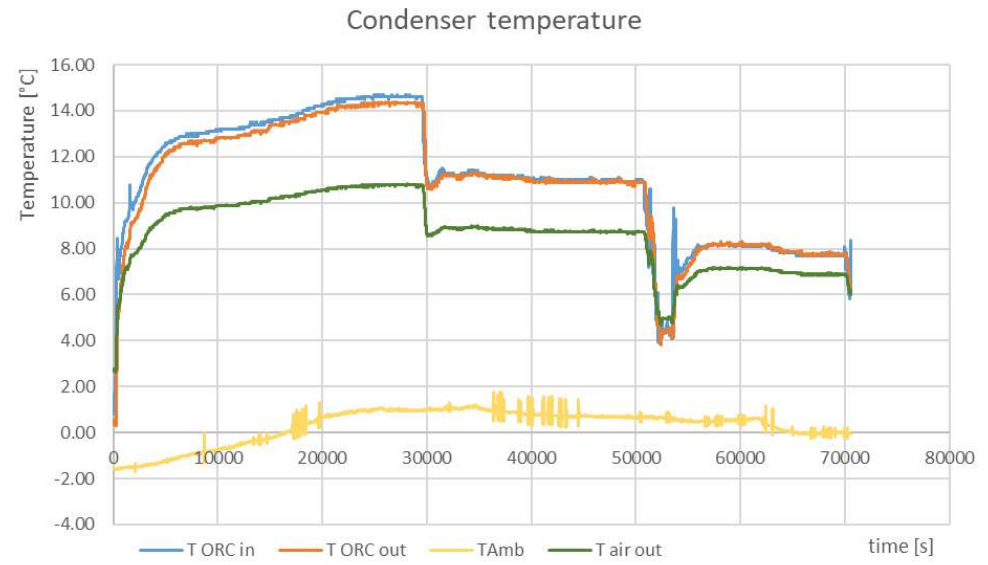

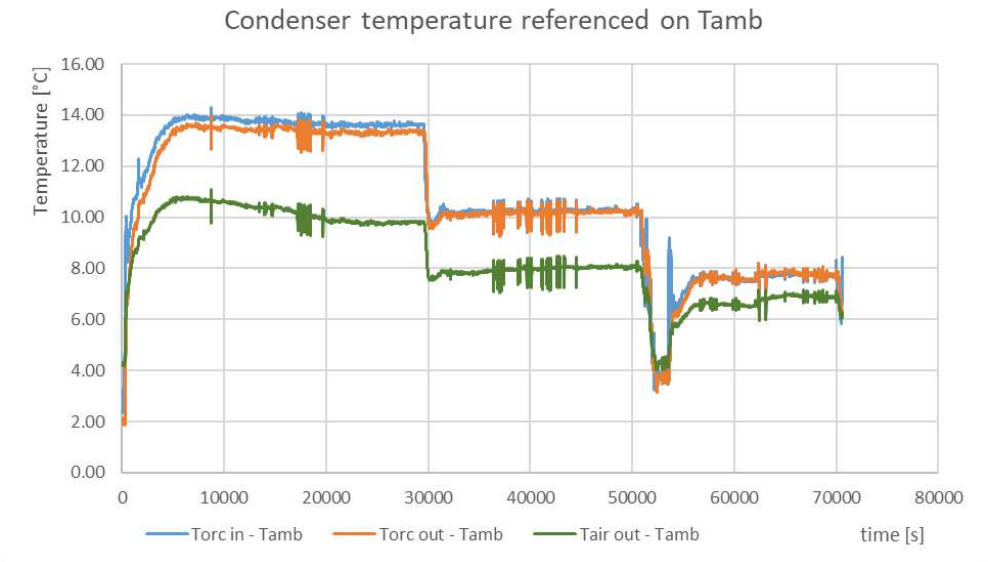

9.6 GESI für MoNiKa

9.6.1 MoNiKa_facility subroutine

This Subprogram for calculates MoNiKa's components characteristics as function of the ORC mass flow

```
function [dP_Hex, MTD_HEx, dP_cond] = MoNiKa_facility(m, mA)

x= m/mA; % mA IS THE DESING MASS FLOW FOR MONIKA FULL LOAD (2.9kg/s)

% Heat Exchanger ======================================================
            Pth = 0.031*x^2 - 0.0017*x + 0.8571;
            Pth = round(Pth,3);

            dP_Hex = 0.022*x^2 + 0.0124*x + 0.0104;
            dP_Hex = round(dP_Hex,3);

            MTD_HEx = -1.684*x+34.868;
            MTD_HEx = round(MTD_HEx,2);

% Condenser ============================================================
            dP_cond  = 0.0007*x^2 + 0.0037*x;
            dP_cond  = round(dP_cond,3);

 end
```

9.6.2 MoNiKa_NETPOWER

This is a subroutine is projected to calculate the real net power of MoNiKa ORC cycle (the thermal water pump consume is not considered). Here is calculated the electrical power consumption of the pumping system and the condenser's Fans. Is valid for supercritical operation, the pumping system was not study for subcritical pressure

At present there is no information on the turbine. In future versions, a study of the electrical power delivered to the grid as function of the ORC mass flow and enthalpy should be performed.

```
function [P_netto_real,P_turb_real,P_pump_real, Grund_vel,LEWA_vel,P_Fans_real, Fan_A,
Fan_Hz, Fan_vel,Tcond_op, etapump, etaturb]= MoNiKa_NETPOWER (P_brutto,
m_air,P_air,T_air, m_orc,mA,Turbinemax,Pumpemax,P3, checkbox4)

%% ======== CONSTANTS ==================================================
Tcond_op =0;            % reserved for future developments
Promass=m_orc/mA;

%  CONDENSER FAN MOTOR(S)
VelMotor = 1460;        %[RPM]
VelFan = 322;           %[RPM]
poles= 4;               % number of poles per phase
etamotorTOT = 0.856;
cos_fi = 0.83;

velRatio = 4.65;
```

```
%% ========================================================================
% ======= solver CONDERNSER ==============================================

rho_air = refpropm('D','T',T_air+273,'P',P_air*1000,'AIR.MIX'); % Density [kg/m^3]
V_air = m_air/rho_air;

V_fan = V_air/3;


    % curves fitted from Manufacturer datasheet
    Pel_fan_op = 0.0001028*V_fan.^3 -0.001272*V_fan.^2 + 0.02344*V_fan + 5.309; % [kW]
    Pfan_axis_op = -4E-05*V_fan.^3 - 0.0006*V_fan.^2 + 0.1851*V_fan + 5.7642; % [kW]
    etafan_tot_op  = -4E-05*V_fan.^4 + 0.0025*V_fan.^3 + 0.0048*V_fan.^2 + 0.085*V_fan +
                                                                        0.2782 ;% [%]

    n_fan = 7.3182*V_fan;           %Afinity Law
    n_motor = n_fan*velRatio;

    A_Fan_op = (Pel_fan_op/(sqrt(3)*400*cos_fi))*1000; %[A] current consume by fan
    hz_Fan_op = n_motor*poles/120;                     %relationship Hz to motor RPM
    Pel_cond_op = Pel_fan_op*3;                        %Total electric power consumption
                                                        by the Fans
    P_Fans_real = round(Pel_cond_op,2);


    % Fan set up for MoNiKa
    Fan_A =  round(A_Fan_op,2);
    Fan_vel= round(n_motor);
    Fan_Hz= round(hz_Fan_op,2);


%% ========================================================================
% ======= solver PUMPING SYSTEM ==========================================

% Main pump (LEWA) ------------------

%case selection for curves range: 5.5, 5.0 and 4.5 MPa are the curves studied
%curves calculation: vel, electrical power consumption and total efficiency

if P3<5.7751 && P3>=5.25
    Pref =5.5;
elseif P3<5.25 && P3>=4.75
    Pref =5.0;
elseif P3<4.75 && P3>=4.25
    Pref = 4.5;
else
    Pref = 0;
end


switch Pref

        case  5.5
             vel_LEWA_op = 444.8*m_orc + 11.63;
             %R-square: 0.9994
             Pel_LEWA_op = Pumpemax*9.7683*m_orc;
             % R-square: 0.9962
             eta_LEWA_op = Pumpemax*0.0335*m_orc^2 - 0.1266*m_orc + 1.0274;   %eta tot
             %R-square: 0.6366


          case  5.0
            vel_LEWA_op = 443.8*m_orc;
            %R-square: 1
            Pel_LEWA_op = Pumpemax*9.8939*m_orc;
            % R-square: 0.1
            eta_LEWA_op = Pumpemax*0.2239*m_orc^2 - 1.0924*m_orc + 2.1529;   %eta tot
            %R-square: 1
```

```
            case  4.5
              vel_LEWA_op = 439.42*m_orc;
              %R-square: 0.9997
              Pel_LEWA_op = Pumpemax*8.984*m_orc;
              %R-square: 0.9995
              eta_LEWA_op  = Pumpemax*0.0088*m_orc^2 - 0.0543*m_orc + 0.9232;   %eta tot
              %R-square: 0.74

          case  0
              str='pressure out of range: 4.5 to 5.5 (+/-5%)  Mpa';
              msgbox(str);
end

% Support pump (Grundfdos) ----------------

              vel_Grundfos_op = 417.29*m_orc + 792.08;
              %R-square: 0.988
              Pel_Grundfos_op = 0.0551*m_orc^3 - 0.2366*m_orc^2 + 0.5769*m_orc - 0.027;
              %R-square: 0.922
              eta_Grundfos_op = -0.0068*m_orc^3 + 0.003*m_orc^2 + 0.0826*m_orc + 0.2077;
              %R-square: 0.709


etapump=(Pel_Grundfos_op/eta_Grundfos_op+Pel_LEWA_op/eta_LEWA_op)/(Pel_Grundfos_op+Pel_LE
WA_op);
etapump =round(etapump);

%-------------------------------------------------------------------------------------------

              %Pumps power characteristic curves
                  q= [1.4:0.1:3.5]; %[m3/s]
                  switch Pref
                      case  5.5
                       P_LEWA = 9.7683*q;
                      case  5.0
                       P_LEWA = 9.8939*q;
                      case  4.5
                      P_LEWA = 8.984*q;
                  end

                  P_Grundfos = 0.0382*q.^3 - 0.1525*q.^2 + 0.4645*q;


    Wpumps_op = Pel_LEWA_op+ Pel_Grundfos_op;
    Grund_vel= round(vel_Grundfos_op);
    LEWA_vel = round(vel_LEWA_op);
    P_pump_real= round(Wpumps_op ,2);


%% ========================================================================
% ======= solver TURBINE ================================================

%not implemented yet.
%here as well as the pumps, a equation of the power delivered to the net as function of
the ORC pressure and mass flow has to be defined.

%in this version it is considered the P burtto and the isentropic efficiency. EtaTurb is
defined by Christian Vetter coefficients, in order to estimate have an estimation.


etaTurb = Turbinemax*(0.652816*(q/mA).^6-3.50172*(q/mA).^5+ 8.25674*(q/mA).^4-
10.3116*(q/mA).^3+ 6.10737*(q/mA).^2-0.211421*(q/mA) +0.00759006);
P_Generated = P_brutto*etaTurb;

etaTurb_op = Turbinemax*(0.652816*Promass^6-3.50172*Promass^5+ 8.25674*Promass^4-
10.3116*Promass^3+ 6.10737*Promass^2-0.211421*Promass +0.00759006);
P_turb_real = P_brutto*etaTurb_op;
P_turb_real= round(P_turb_real,2);
```

```
etaturb = etaTurb_op;
etaturb = round(etaturb,2)*100;

%% %%%%%%%%%%%%%%%%%%%%%%%%%%%%%%%%%%%%%%%%%%%%%%%%%%%%%%%%%%%%%%%%%%%%%%%%
% ======= solver Power consumption ======================================

% Calculation of Real net power generation

P_consume_tot = Pel_cond_op + Pel_LEWA_op + Pel_Grundfos_op;
P_netto_real = P_turb_real-P_consume_tot;  %

    P_netto_real=round( P_netto_real ,2);


end
```